NATIONAL ADVISORY COMMITTEE FOR AERONAUTICS

TECHNICAL NOTE

No. 1226

THEORETICAL SUPERSONIC LIFT AND DRAG CHARACTERISTICS OF SYMMETRICAL WEDGE-SHAPE-AIRFOIL SECTIONS AS AFFECTED BY SWEEPBACK OUTSIDE THE MACH CONE

By H. Reese Ivey and Edward N. Bowen, Jr.

Langley Memorial Aeronautical Laboratory
Langley Field, Va.

Washington
March 1947

NATIONAL ADVISORY COMMITTEE FOR AERONAUTICS

TECHNICAL NOTE NO. 1226

THEORETICAL SUPERSONIC LIFT AND DRAG CHARACTERISTICS OF SYMMETRICAL WEDGE-SHAPE-AIRFOIL SECTIONS AS AFFECTED BY SWEEPBACK OUTSIDE THE MACH CONE

By H. Reese Ivey and Edward N. Bowen, Jr.

SUMMARY

The theoretical supersonic section lift and drag characteristics of thin, wedge-shape, untapered airfoils with sweepback are presented. The results apply to those parts of the wing in two-dimensional flow and are not applicable to wings swept back within the Mach cone of the center section. The results may also be applied to swept-forward wings if the angle of sweep is not enough to put the wing within the Mach cone from the tips.

INTRODUCTION

A simplified method is presented in reference 1 for determining the pressure distribution around thin, sharp-nose airfoils at supersonic speeds. This method considers the entropy increase through the shock waves and calculates the pressure changes through the shock and expansion waves. The method was shown to be accurate for wedge-shape airfoils and to give a close approximation for continuously curving airfoils. The calculated pressure distribution was shown to check the experimental distribution at low Reynolds numbers except for a small region of separated flow near the trailing edge. The type of flow encountered when extreme sweepback (within the Mach cone) is used at supersonic speeds is discussed in reference 4. In that report it was shown that low drag coefficients could be obtained when the wing was swept back sufficiently to make the velocity component perpendicular to the leading edge of the wing subsonic. Experimental results at higher Reynolds numbers show that the region of breakaway becomes negligible as the Reynolds number increases and hence the calculations should be accurate for full-scale aircraft.

Reference 2 used the method of reference 1 to calculate the characteristics of thin double-wedge airfoils at supersonic speeds.

The section characteristics for wing sections swept back outside the Mach cone were first determined by Busemann in reference 3. In that paper the component theory was introduced and used to calculate some of the airfoil characteristics of swept-back wings.

The present paper extends the work of Busemann (reference 3) and makes use of the component theory in conjunction with the method of reference 1 to determine the section lift and drag characteristics of swept-back double-wedge-airfoil sections. A brief discussion is included of the trends indicated by the results.

SYMBOLS

a	speed of sound in air, feet per second
c_d	section pressure-drag coefficient
c_l	section lift coefficient
M	Mach number
t	thickness of airfoil section, feet
c	length of chord, feet
u	component of free-stream velocity normal to plane of shock
v	component of free-stream velocity in plane of shock
$\Delta p/q$	pressure coefficient
Δp	difference between local static pressure and free-stream static pressure
q	dynamic pressure
p_1	static pressure on upper leading edge of airfoil
p_2	static pressure on upper trailing edge of airfoil
p_3	static pressure on lower leading edge of airfoil
p_4	static pressure on lower trailing edge of airfoil
γ	ratio of specific heats

L lift

D drag

$\frac{dc_l}{d\alpha}$ slope of lift curve

α angle of attack, degrees

β angle through which flow turns (that is, change in surface angle of airfoil), degrees

Λ sweep angle, degrees

ϕ half angle of airfoil, degrees

ψ Mach angle, degrees

Subscripts:

a after shock

b before shock

o measured in free-stream direction

e measured perpendicular to leading edge

T total

M = 1 for the flow condition when Mach number equals unity

M = 0 for the flow condition when Mach number equals zero

THEORETICAL CONSIDERATIONS

The equations of Meyer as given in reference 5 show that the velocity components normal to any plane shock (herein designated u_b, before shock, and u_a, after shock) are related to the speed of sound before the shock corresponding to a Mach number of unity and the free-stream-velocity component in the plane of the shock by the following equation:

$$u_b u_a = \left(a_{M=1}\right)^2 - \frac{\gamma - 1}{\gamma + 1} v^2$$

where

$a_{M=1}$ speed of sound corresponding to a Mach number of unity before shock $\left((a_{M=0})\sqrt{\frac{2}{\gamma+1}}\right)$

v component of free-stream velocity in plane of shock

$a_{M=0}$ stagnation speed of sound before shock

Since

$$(a_{M=0})^2 = a_b^2\left(1 + \frac{\gamma - 1}{2} M_b^2\right)$$

and

$$a_b^2 M_b^2 = u_b^2 + v^2$$

it follows that

$$u_b u_a = \frac{2a_b^2}{\gamma + 1} + \frac{\gamma - 1}{\gamma + 1} u_b^2$$

From this relation it can be seen that, for a given value of local speed of sound before the shock a_b, the change of state across a plane shock is determined only by the free-stream-velocity component normal to the shock plane u_b. This fact is useful in calculating the theoretical section pressure distributions of the swept-back wings considered herein.

The obvious limitations to the method are that the wing section considered must not be swept back within the Mach cone of the center section and that the wing section should not exceed the limits illustrated in figures 3 and 4 of reference 1.

For the present study the free-stream-velocity vector is broken into components, one of which is parallel to the leading edge of the wing and is therefore in the plane of the attached shock wave. Since this component of free-stream velocity has been shown to have no effect on the change of state across the shock,

the pressure distributions can be calculated from the velocity vectors normal to the leading edge.

For wings swept back outside the Mach cone a part of the wing is, effectively, in two-dimensional flow. Figure 1 defines the zones of two-dimensional flow for the wing plan forms considered in the present paper. The part of the wing lying in the central and tip areas indicated in figure 1 will have considerable three-dimensional flow. The calculations presented are valid only for the part of the wing in two-dimensional flow. The characteristics of a swept-back wing of finite aspect ratio (tips and center section being considered) can be approximated by a combination of the results presented herein and the linearized method of reference 6. The calculations presented herein are suitable for swept-forward as well as swept-back wings. In order to illustrate the effect of sweepback on lift and drag, a simplified analysis of the flow over the example wing shown in figure 2 will be discussed first. For this example, the wing is assumed to be operating under the following conditions:

Free-stream Mach number, M_o	4
Angle of attack, α_o, degrees	1
Thickness ratio perpendicular to the leading edge, $\left(\frac{t}{c}\right)_e$	0.05
Sweepback angle, Λ, degrees	60

Figure 2 gives plane and side elevation views of the example wing for the operating conditions specified. Figure 2 differentiates between two methods of measuring section thickness ratio; namely, perpendicular to leading edge (section A-A) or parallel to free-stream direction (section B-B). In general, all calculations are carried out for values of $\left(\frac{t}{c}\right)_o = 0.05$ and $\left(\frac{t}{c}\right)_e = 0.05$ and 0.10. The subscript "e" signifies effective and indicates that the component is measured perpendicular to the leading edge and the subscript "o", that the component is measured in the direction of the free-stream velocity. In order to make the calculations the free-stream Mach number vector is broken into three components: M_1 perpendicular to the leading edge and lying in the plane determined by the chord lines, M_2 perpendicular to the plane determined by the chord lines, and M_3 parallel to the leading edge. Except for tip effects, which do not influence the section being studied, the flow parallel to the leading edge does not affect the pressure distribution and hence will be neglected.

In order to expedite the calculations for the illustrative example, some simplified equations are used instead of the exact equations which are given in the appendix. It must be emphasized that the approximate method has been used only in the illustrative example.

For small angles of attack

$$M_1 \approx M_o \cos \Lambda \approx 2$$

and

$$M_2 = M_o \sin \alpha_o$$

Now an effective angle of attack α_e is based on M_1 and M_2 instead of M_o. The vector sum of M_1 and M_2 is effective free-stream Mach number M_e. The effective angle of attack α_e is then

$$\alpha_e = \arctan \frac{M_2}{M_1} \approx \arctan M_o \sin \frac{\alpha_o}{M_o} \cos \Lambda$$

For small angles of attack, sin α_o and tan α_o may be replaced by α_o. Then

$$\alpha_e = \arctan \frac{\alpha_o}{\cos \Lambda} \approx 2^\circ$$

and since $M_e = \sqrt{M_1^2 + M_2^2} \approx M_1$, the problem has been simplified to the extent that the lift and drag characteristics of an unswept wing section at 2° angle of attack and Mach number 2 can be used. Reference 2 gives the pressure drag coefficient of this airfoil as

$$c_d = 0.0085$$

and the lift coefficient as

$$c_l = 0.082$$

These coefficients are based on the dynamic pressure corresponding to M_e. In order to base them on M_o the coefficients must be multiplied by $\left(\frac{M_e}{M_o}\right)^2 = \cos^2\Lambda$. It must also be remembered that only one component, $c_d \cos\Lambda$, of the drag force is in the free-stream direction; consequently, the lift and pressure-drag coefficients based on free-stream conditions become

$$c_{l_o} = 0.082 \times 0.5^2 = 0.0205$$

$$c_{d_o} = 0.0085 \times 0.5^3 = 0.00106$$

Some allowance must be made for skin friction, which is changed only by a Reynolds number effect due to the sweepback. The exact nature of supersonic skin-friction drag is not as yet completely defined but for the present analysis its effect can be shown by assuming that the supersonic skin-drag coefficient remains constant in the supersonic range at a reasonable subsonic value. If the effect of a skin-friction coefficient other than the value assumed herein is desired, the curves presented in this paper may be shifted accordingly. For this example the skin-friction drag coefficient is assumed to be 0.006 and the total drag coefficient is

$$c_{d_T} = 0.006 + 0.00106 = 0.00706$$

The pressure drag is thus only a small part of the total drag. Reference 2 may be used to determine the section lift and drag coefficients of an unswept wing with a thickness ratio of 5 percent when thickness is measured perpendicular to leading edge for $\alpha_o = 1^\circ$ and $M_o = 4$. These data may be compared with the swept-back-wing section coefficients, as follows:

	Swept-back wing, $\Lambda = 60^\circ$	Unswept wing
c_{d_T}	0.00706	0.00900
c_l	0.0205	0.0180

In this particular case the addition of sweepback increased the lift and decreased the drag of the section. It must be remembered, however, that this example serves only to point out the problems involved in calculating the airfoil characteristics of swept-back wings and is not intended to lead to any particular conclusions as to the general advantage of sweepback. Some of the equations used for this illustrative example are approximations which do not apply at high angles of attack. The exact equations used in the paper are cumbersome and hence are presented in the appendix in order that the main body of the paper not be unnecessarily complicated.

PRESENTATION OF RESULTS

Slope of the lift curve.- Reference 2 has shown that the slope of the lift curve decreases as the Mach number increases above 1.0. It can be expected, therefore, that the addition of sweepback at high supersonic speeds will tend to increase the lift by making the effective Mach number approach 1 and by increasing the effective angle of attack but will tend to decrease the lift by decreasing the effective dynamic pressure. The resultant effect depends on the actual speeds and angles involved.

Figure 3 presents the variation with the sweepback of the slope of the section lift curves (based on free-stream angles of attack and free-stream lift coefficients) for a wing section of 5-percent effective thickness ratio. Curves are given for constant values of free-stream Mach number. The curves show that at low supersonic speeds substantial increases in the slope of the lift curve are the result of increasing angle of sweepback. For example, at $M_o = 1.5$, $\frac{dc_{l_o}}{d\alpha_o} = 0.0630$ for $\Lambda = 0^\circ$ and $dc_{l_o}/d\alpha_o$ has increased to a value of 0.0735 for $\Lambda = 30^\circ$. However, at higher forward Mach numbers the slope of the lift curve does not change appreciably with increasing sweepback until the sweepback is sufficient to reduce the effective Mach number to the vicinity of unity.

Since reference 2 has shown that thickness ratio has no appreciable effect on the slope of the lift curve, figure 3 has been limited to a single value of thickness ratio.

Minimum drag coefficient.- The effect of sweepback on the section minimum drag coefficients is shown in figure 4.

If the thickness ratio measured in the free-stream direction is held constant, the section minimum drag coefficient will in general increase slightly with an increase in sweepback. If the effective thickness ratio is held constant, the drag coefficient may decrease appreciably before increasing. This decrease is evident at Mach numbers considerably greater than unity. (See fig. 4(a) at $M_o = 8$.)

Ratio of section lift to drag.- The ratio of section lift to section drag has been selected as the parameter which represents most clearly the effectiveness of an airfoil section acting as a lifting device. This parameter has been calculated and plotted as a function of section lift coefficient c_l for various combinations of Λ, $\frac{t}{c}$, and M_o. (See table I.) The results include both the pressure drag and total drag. It should be noted that, wherever a combination of Λ, c_{l_o}, and M_o resulted in a value of effective Mach number M_e less than the minimum value for which application of the method of reference 1 is considered valid, the curves were either omitted or restricted in extent. For operating conditions approaching these limits and with a wing of finite aspect ratio, the portion of the wing for which these calculations are valid is a small percentage of the total wing area.

An examination of figures 5 through 16 yields the following general trends:

(1) For a given combination of M_o and $\left(\frac{t}{c}\right)_e$ an increase in the sweepback angle substantially increases the values of maximum $\frac{c_{l_o}}{c_{d_o}}$ and $\frac{c_{l_o}}{c_{d_o} + 0.006}$.

(2) For a given combination of M_o and $\left(\frac{t}{c}\right)_o$ an increase in the sweepback angle does not appreciably affect the value of maximum $\frac{c_{l_o}}{c_{d_o}}$ or $\frac{c_{l_o}}{c_{d_o} + 0.006}$.

(3) For a given combination of M_o and $\left(\frac{t}{c}\right)_e$ or $\left(\frac{t}{c}\right)_o$ an increase in the sweepback angle has no appreciable effect on the value of c_{l_o} for maximum $\frac{c_{l_o}}{c_{d_o}}$ or $\frac{c_{l_o}}{c_{d_o} + 0.006}$.

(4) For a given combination of Λ and $\left(\frac{t}{c}\right)_e$ or $\left(\frac{t}{c}\right)_o$ an increase in the operating free-stream Mach number substantially decreases the value of c_{l_o} for maximum $\frac{c_{l_o}}{c_{d_o}}$ or $\frac{c_{l_o}}{c_{d_o} + 0.006}$.

(5) For a given combination of Λ and $\left(\frac{t}{c}\right)_e$ or $\left(\frac{t}{c}\right)_o$ an increase in the operating free-stream Mach number decreases the value of maximum $\frac{c_{l_o}}{c_{d_o} + 0.006}$ but has no appreciable effect on the value of maximum $\frac{c_{l_o}}{c_{d_o}}$.

It may be of interest to compare the exact results of the present paper with the approximate formulas developed from the linearized supersonic theory. The linearized theory is, of course, restricted to thin airfoils at small angles of attack and at stream Mach numbers large enough to give an attached shock.

By use of the component theory the approximate formulas for determining the characteristics of the ratio of maximum lift to pressure drag of swept-back sections are

$$\left(\frac{L}{D}\right)_{max} = \frac{1}{2 \cos \Lambda}\left(\frac{c}{t}\right)_e$$

$$\alpha_o = \left(\frac{t}{c}\right)_e \cos \Lambda$$

$$c_{l_o} = \frac{4\left(\frac{t}{c}\right)_e \cos^2 \Lambda}{\sqrt{(M_o \cos \Lambda)^2 - 1}}$$

These formulas provide close approximation to the exact values of the present paper within the limits of their application.

It is evident that for both swept-back and unswept wedge-shape sections the maximum ratio of lift to pressure drag occurs when two sides of the wing section are parallel to the direction of flight.

CONCLUSIONS

The calculated results presented in this paper indicate that:

1. Increasing sweepback at a constant stream Mach number increases the value of the ratio of lift to pressure drag and the ratio of lift to total drag, provided that the thickness ratio measured in the free-stream direction is allowed to decrease.

2. Increasing sweepback at a constant stream Mach increases the slope of the lift curve substantially except at high stream Mach numbers where the effect is negligible.

3. Increasing sweepback at a constant stream Mach number decreases the minimum drag coefficient provided the free-stream thickness ratio is allowed to decrease.

4. The section lift coefficient for the maximum ratio of lift to pressure drag and of lift to total drag decreases with an increase in free-stream Mach number regardless of sweepback.

5. The approximate linearized solution for the lift and drag characteristics of a swept-back wing section at the maximum value of the ratio of lift to pressure drag agree well with the exact values of the present paper provided that: (a) the airfoil is thin, (b) the airfoil is at a small angle of attack, and (c) the free-stream Mach number is well above the minimum value for an attached shock.

Langley Memorial Aeronautical Laboratory
National Advisory Committee for Aeronautics
Langley Field, Va., September 20, 1946

APPENDIX

METHOD OF COMPUTATION

The following formulas are derived by the application of trigonometry and analytic geometry to the basic wing sections considered. (See fig. 2.)

The effective Mach number M_e which is the component of the free-stream Mach number M_o acting perpendicular to the leading edge, is expressed in terms of the angle of sweepback Λ and the free-stream angle of attack α_o as

$$M_e = M_o\sqrt{1 - \sin^2\Lambda \cos^2\alpha_o}$$

where

M_e effective Mach number; that is, the component of M_o acting perpendicular to the leading edge

The effective Mach number M_e can be further broken up into

(a) The component of M_e (and therefore also of M_o) lying in the plane of the chord lines and perpendicular to the leading edge given by $M_o \cos \alpha_o \cos$

(b) The component of M_e (and therefore also of M_o) perpendicular to the plane of the chord lines, given by $M_o \sin \alpha_o$

The effective angle of attack, that is, the angle of attack of the airfoil section measured perpendicular to the leading edge, is

$$\alpha_e = \arctan \frac{\tan \alpha_o}{\cos \Lambda}$$

and the effective thickness ratio, that is, the thickness ratio measured perpendicular to the leading edge, is

$$\left(\frac{t}{c}\right)_e = \frac{\left(\frac{t}{c}\right)_n}{\cos \Lambda}$$

If ϕ_e is the half-angle of the airfoil measured perpendicular to the leading edge and β_e is the angle through which the flow turns (that is, change in surface angle of airfoil) measured in the plane perpendicular to leading edge, then

$$\phi_e = \alpha_e + \beta_e = \arctan \frac{\left(\frac{t}{c}\right)_o}{\cos \Lambda}$$

Pressure coefficients $\frac{\Delta p}{q_e}$ are now determined by the method of reference 1 for the effective airfoil section operating at the effective angle of attack and at the effective Mach number. These pressure coefficients are then converted to lift and drag section coefficients based on free-stream measurements by the following formulas:

$$c_{d_o} = \frac{1}{2}\left(\frac{M_e}{M_o}\right)^2 \left\{ \left[\frac{\Delta p_1}{q_e} - \frac{\Delta p_4}{q_e}\right]\left[\left(\frac{t}{c}\right)_o \cos \alpha_o - \sin \alpha_o\right] \right.$$

$$\left. + \left[-\frac{\Delta p_1}{q_e} + \frac{\Delta p_4}{q_e}\right]\left[\left(\frac{t}{c}\right)_o \cos \alpha_o + \sin \alpha_o\right] \right\}$$

$$c_{l_o} = \frac{1}{2}\left(\frac{M_e}{M_o}\right)^2 \left\{ \left[-\frac{\Delta p_1}{q_e} + \frac{\Delta p_4}{q_e}\right]\left[\left(\frac{t}{c}\right)_o \sin \alpha_o + \cos \alpha_o\right] \right.$$

$$\left. + \left[-\frac{\Delta p_2}{q_e} + \frac{\Delta p_3}{q_e}\right]\left[-\left(\frac{t}{c}\right)_o \sin \alpha_o + \cos \alpha_o\right] \right\}$$

where the subscripts 1 and 2 refer to the leading and trailing parts, respectively, of the upper surface of the airfoil and the subscripts 3 and 4 refer to the leading and trailing parts, respectively, of the lower surface.

REFERENCES

1. Ivey, H. Reese, Stickle, George W., and Schuettler, Alberta: Charts for Determining the Characteristics of Sharp-Nose Airfoils in Two-Dimensional Flow at Supersonic Speeds. NACA TN No. 1143, 1947.

2. Ivey, H. Reese: Notes on the Theoretical Characteristics of Two-Dimensional Supersonic Airfoils. NACA TN No. 1179, 1947.

3. Busemann, A.: Aerodynamic Lift at Supersonic Speeds. 2844, Ae. Techl. 1201, British A.R.C., Feb. 3, 1937. (From Luftfahrtforschung, Bd. 12, Nr. 6, Oct. 3, 1935, pp. 210-220.)

4. Jones, Robert T.: Wing Plan Forms for High-Speed Flight. NACA TN No. 1033, 1946.

5. Ackeret, J.: Gasdynamik. Handbuch d. Physik, Bd. VII, Kap. 5, Julius Springer (Berlin), 1927, p. 330.

6. Jones, Robert T.: Thin Oblique Airfoils at Supersonic Speed. NACA TN No. 1107, 1946.

TABLE I. - PRESENTATION OF RESULTS

Figure	Parameters	$\left(\frac{t}{c}\right)_e$	$\left(\frac{t}{c}\right)_o$	Λ (deg)	M_o
[a] 4(a)	Λ against c_{d_o}	0.10	----	-------	1.5 to 8
(b)		.05	----	-------	1.5 to 8
(c)		----	0.05	-------	1.5 to 8
5(a)	c_{l_o} against $\frac{c_{l_o}}{c_{d_o}}$	.10	----	0	1.5 to 8
(b)		.10	----	15	1.5 to 8
(c)		.10	----	30	2 to 8
(d)		.10	----	45	2 to 8
(e)		.10	----	60	4 to 8
6(a)	c_{l_o} against $\frac{c_{l_o}}{c_{d_o}}$	.10	----	0 to 15	1.5
(b)		.10	----	0 to 45	2
(c)		.10	----	0 to 60	4
(d)		.10	----	0 to 60	8
7(a)	c_{l_o} against $\frac{c_{l_o}}{c_{d_o} + 0.006}$	.10	----	0	1.5 to 8
(b)		.10	----	15	1.5 to 8
(c)		.10	----	30	2 to 8
(d)		.10	----	45	2 to 8
(e)		.10	----	60	4 to 8
8(a)	c_{l_o} against $\frac{c_{l_o}}{c_{d_o} + 0.006}$	.10	----	0 to 30	1.5
(b)		.10	----	0 to 45	2
(c)		.10	----	0 to 60	4
(d)		.10	----	0 to 60	8
9(a)	c_{l_o} against $\frac{c_{l_o}}{c_{d_o}}$	.05	----	0	1.5 to 8
(b)		.05	----	15	1.5 to 8
(c)		.05	----	30	1.5 to 8
(d)		.05	----	45	2 to 8
(e)		.05	----	60	4 to 8
10(a)	c_{l_o} against $\frac{c_{l_o}}{c_{d_o}}$	.05	----	0 to 30	1.5
(b)		.05	----	0 to 45	2
(c)		.05	----	0 to 60	4
(d)		.05	----	0 to 60	8

[a]Angle of attack, $\alpha = 0^\circ$

TABLE I. - PRESENTATION OF RESULTS - Concluded

Figure	Parameters	$\left(\frac{t}{c}\right)_e$	$\left(\frac{t}{c}\right)_o$	Λ (deg)	M_o
11(a)	c_{l_o} against $\frac{c_{l_o}}{c_{d_o} + 0.006}$	0.05	----	0	1.5 to 8
(b)		.05	----	15	1.5 to 8
(c)		.05	----	30	1.5 to 8
(d)		.05	----	45	2 to 8
(e)		.05	----	60	4 to 8
12(a)	c_{l_o} against $\frac{c_{l_o}}{c_{d_o} + 0.006}$	.05	----	0 to 30	1.5
(b)		.05	----	0 to 45	2
(c)		.05	----	0 to 60	4
(d)		.05	----	0 to 60	8
13(a)	c_{l_o} against $\frac{c_{l_o}}{c_{d_o}}$	----	.05	0	1.5 to 8
(b)		----	.05	15	1.5 to 8
(c)		----	.05	30	1.5 to 8
(d)		----	.05	45	2 to 8
(e)		----	.05	60	4 to 8
14(a)	c_{l_o} against $\frac{c_{l_o}}{c_{d_o}}$	----	.05	0 to 30	1.5
(b)		----	.05	0 to 45	2
(c)		----	.05	0 to 60	4
(d)		----	.05	0 to 60	8
15(a)	c_{l_o} against $\frac{c_{l_o}}{c_{d_o} + 0.006}$	----	.05	0	1.5 to 8
(b)		----	.05	15	1.5 to 8
(c)		----	.05	30	1.5 to 8
(d)		----	.05	45	2 to 8
(e)		----	.05	60	4 to 8
16(a)	c_{l_o} against $\frac{c_{l_o}}{c_{d_o} + 0.006}$	----	.05	0 to 30	1.5
(b)		----	.05	0 to 45	2
(c)		----	.05	0 to 60	4
(d)		----	.05	0 to 60	8

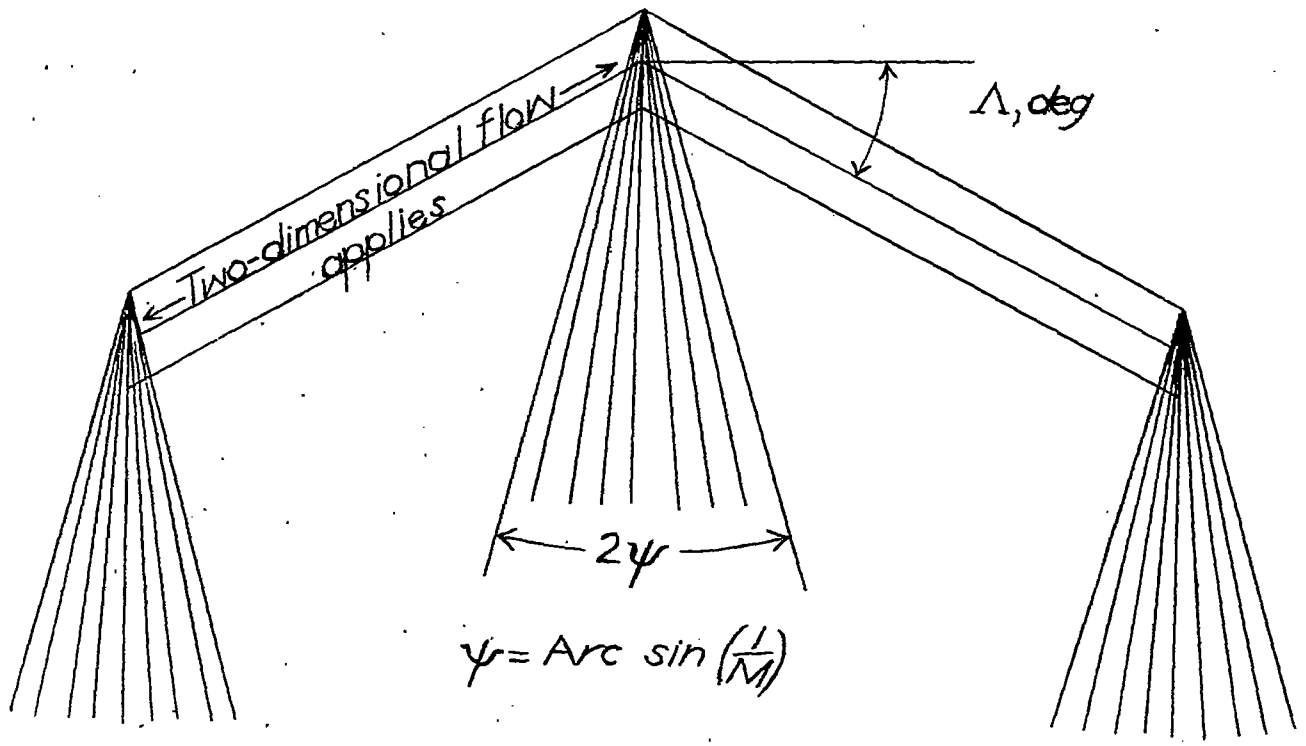

NATIONAL ADVISORY
COMMITTEE FOR AERONAUTICS

Figure 1.- Zones of two-dimensional-flow application.

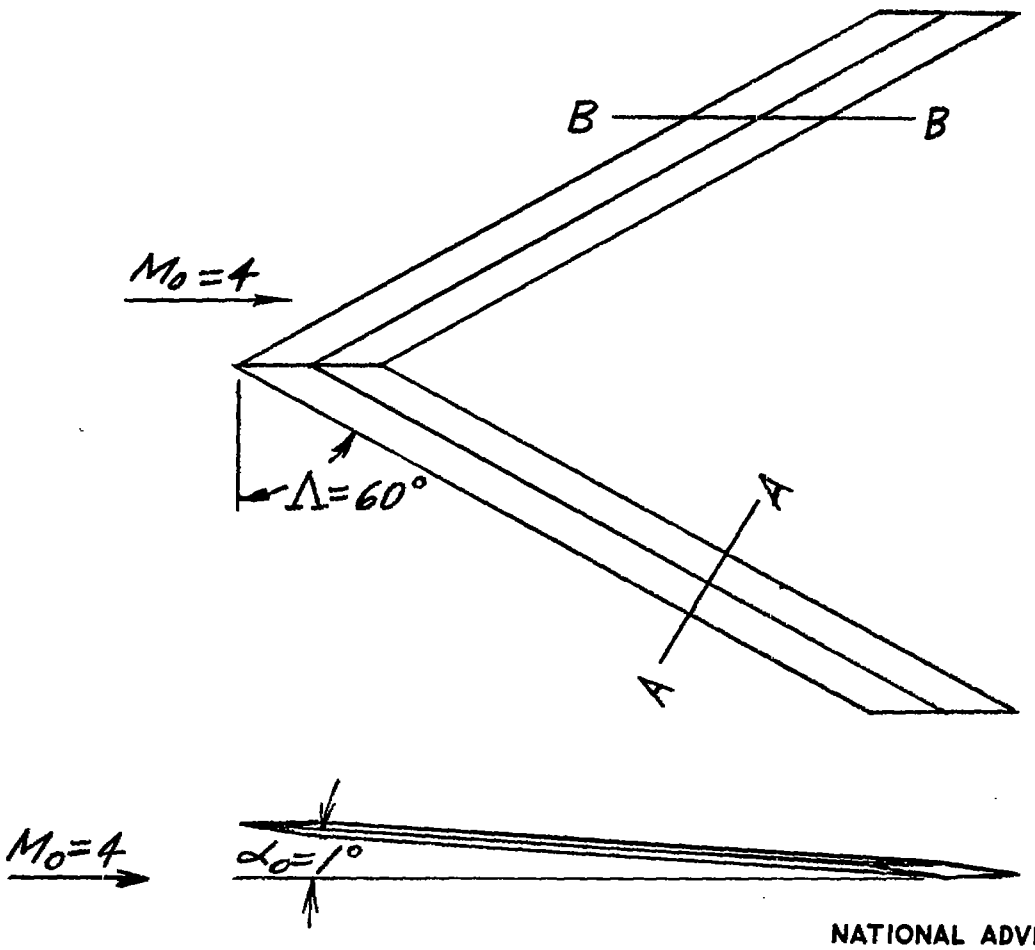

Figure 2.- Example wing.

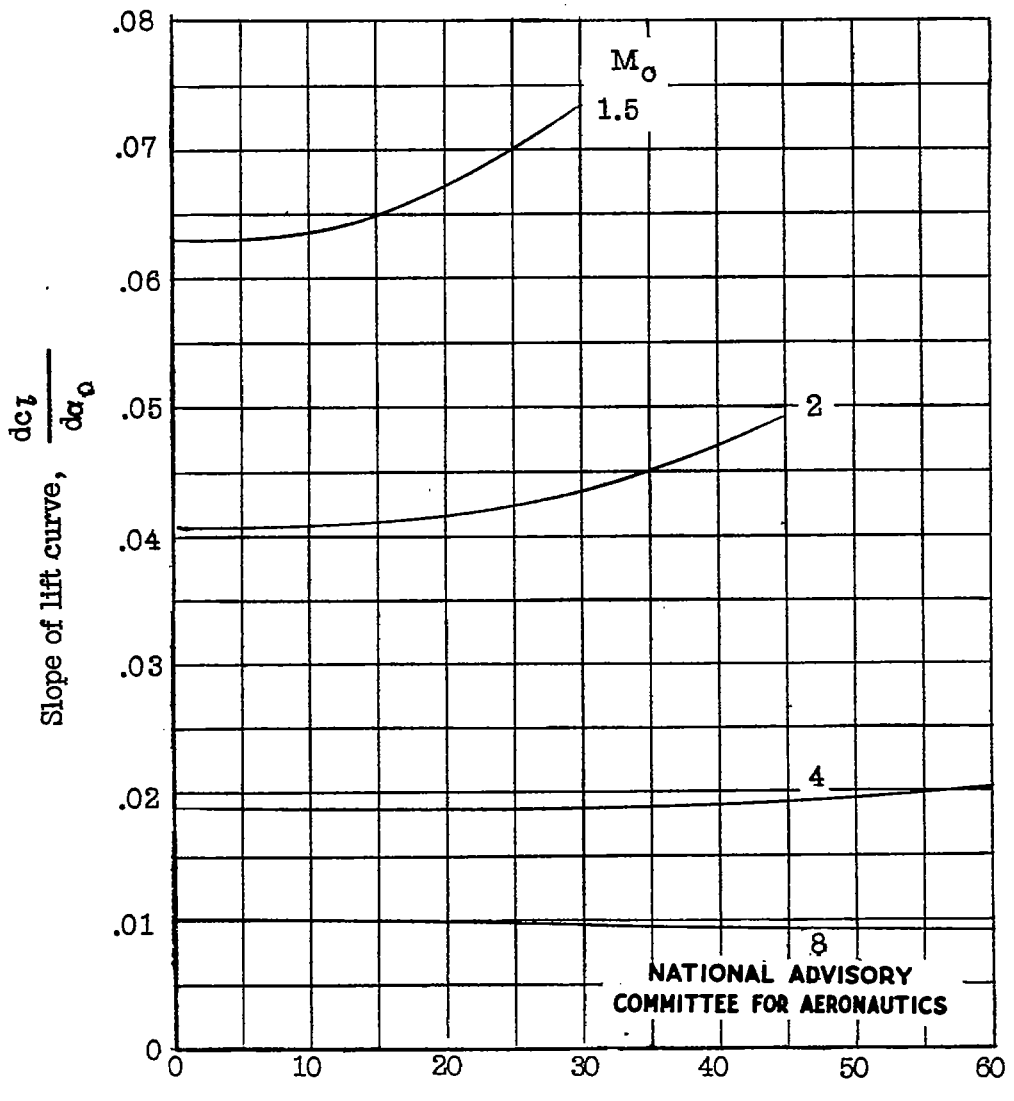

Figure 3.- Effect of sweepback on the slope of the lift curve. $\alpha_o = 0^\circ$, $\left(\frac{t}{c}\right)_e = 0.05$.

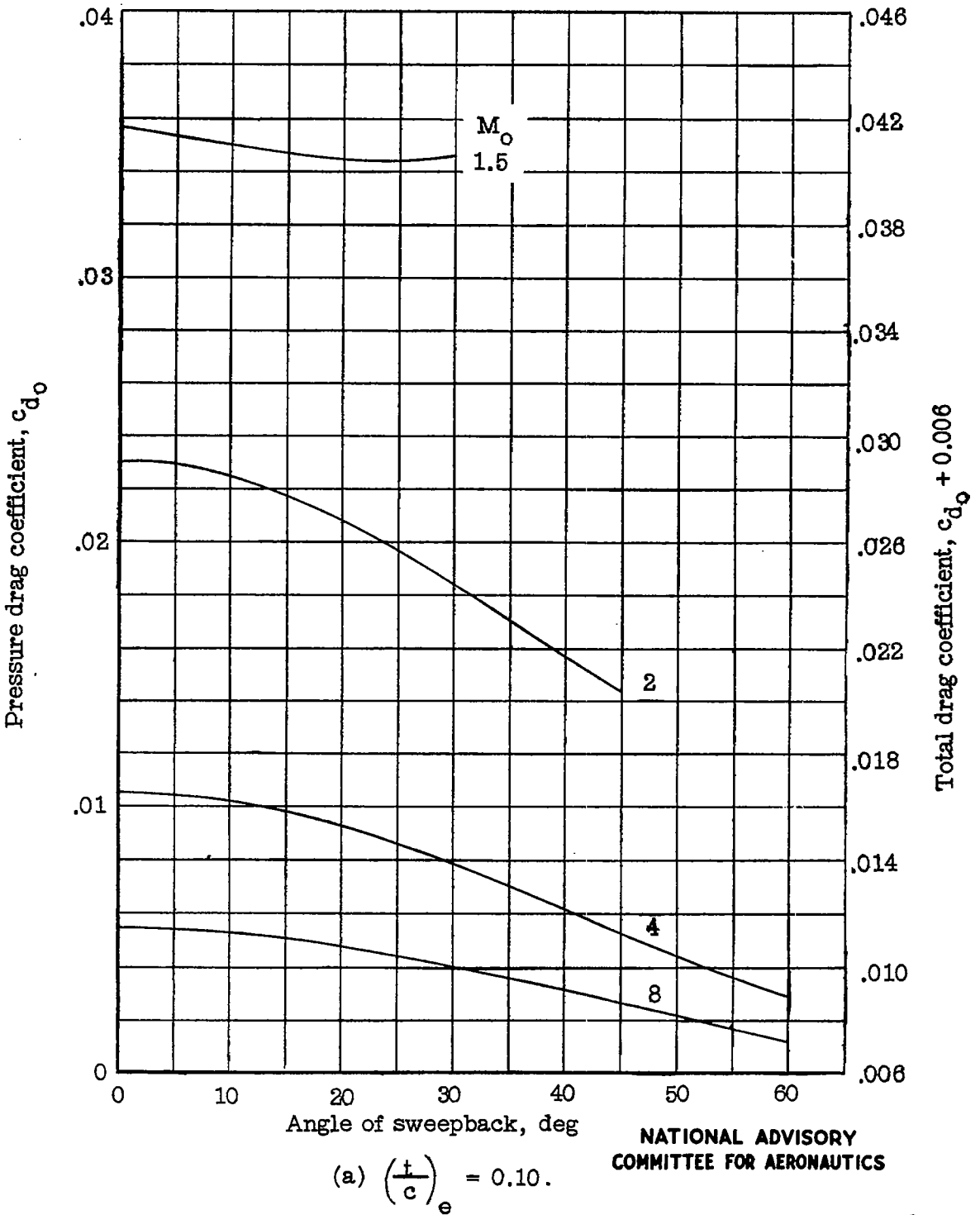

(a) $\left(\frac{t}{c}\right)_e = 0.10$.

Figure 4.- Effect of sweepback on minimum drag coefficient. $\alpha_o = 0^o$.

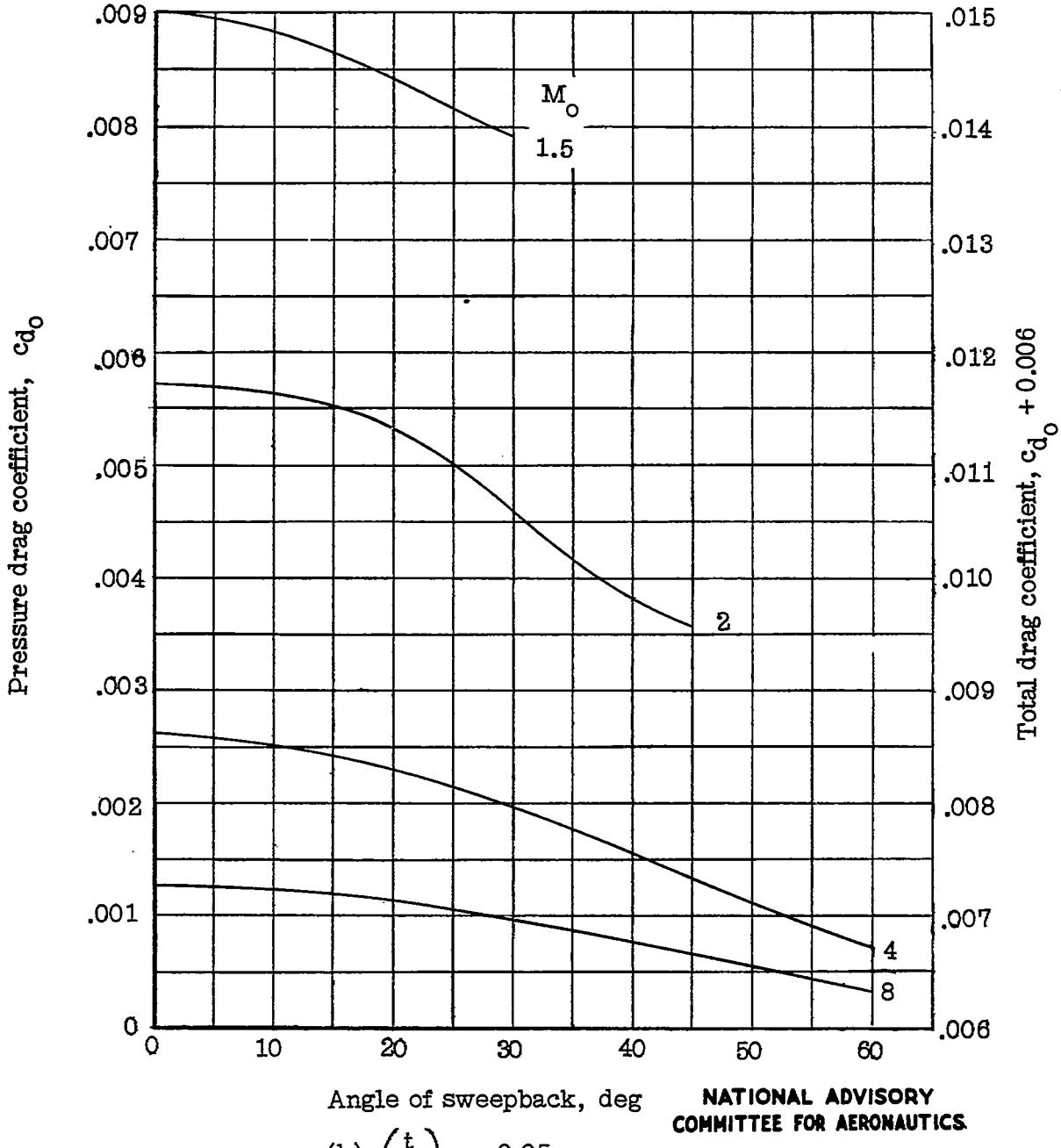

(b) $\left(\frac{t}{c}\right)_e = 0.05$.

Figure 4.- Continued.

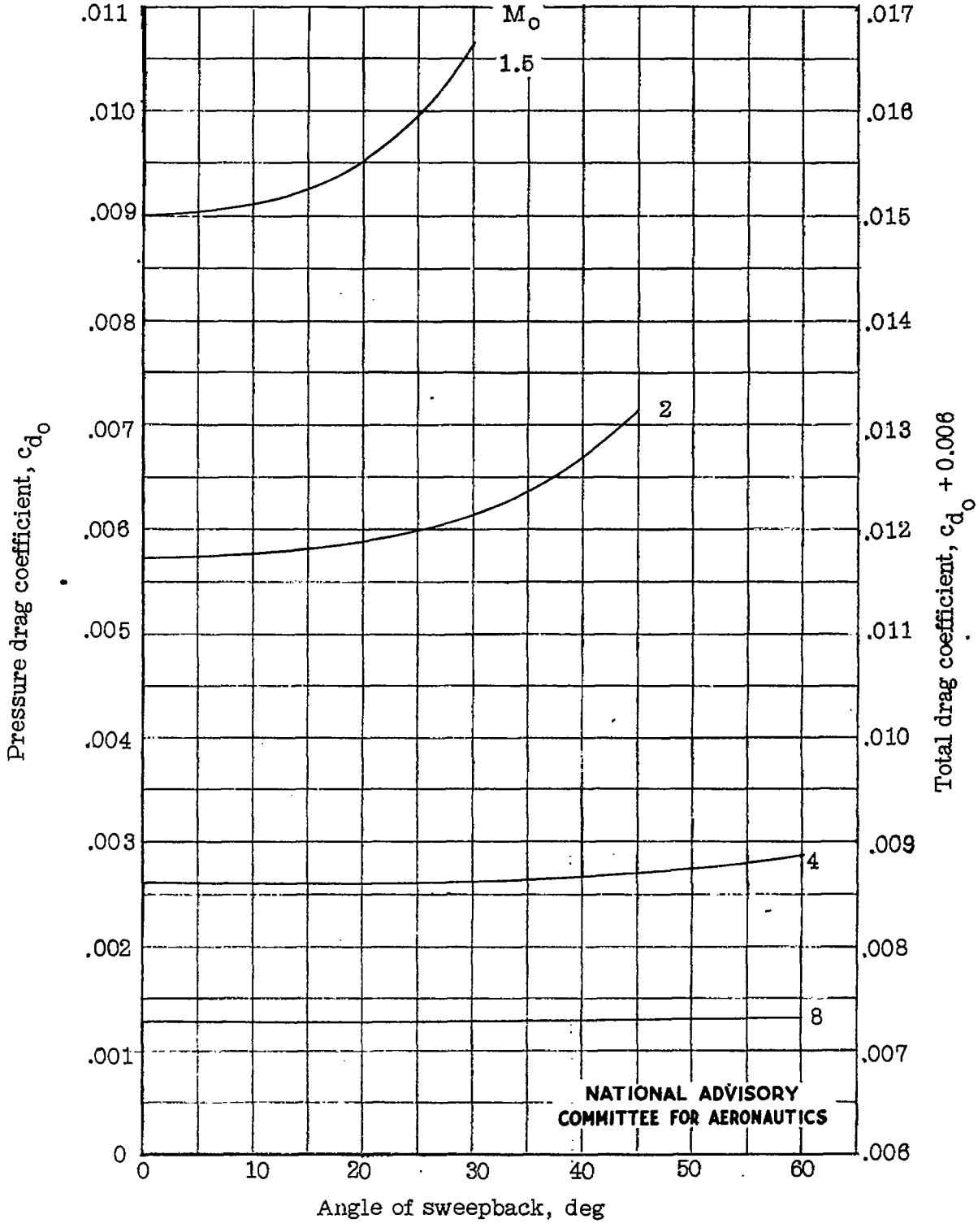

(c) $\left(\frac{t}{c}\right)_o = 0.05$.

Figure 4.- Concluded.

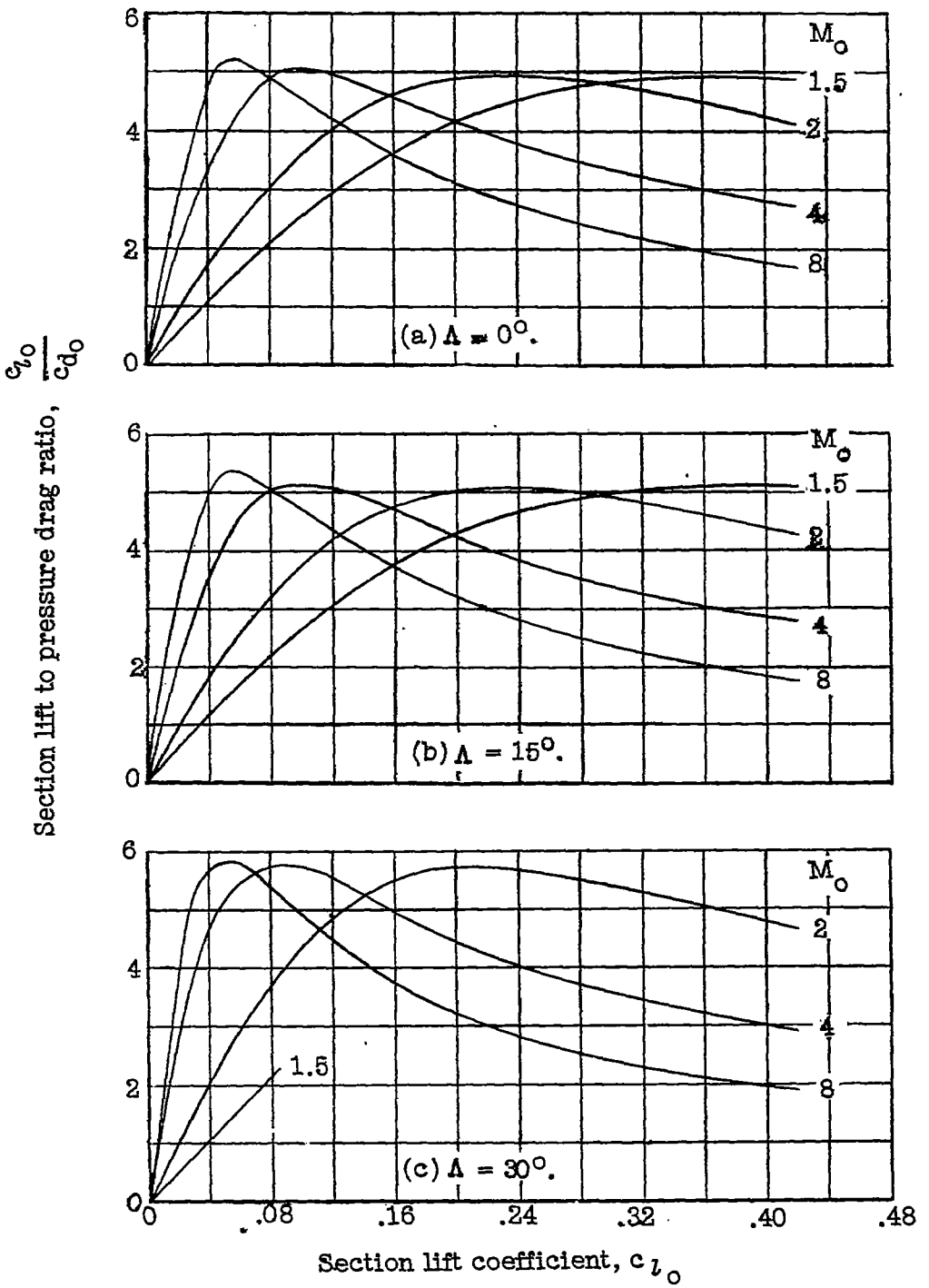

NATIONAL ADVISORY COMMITTEE FOR AERONAUTICS

Figure 5.- Ratio of lift to pressure drag; $\left(\frac{t}{c}\right)_e = 0.10$.

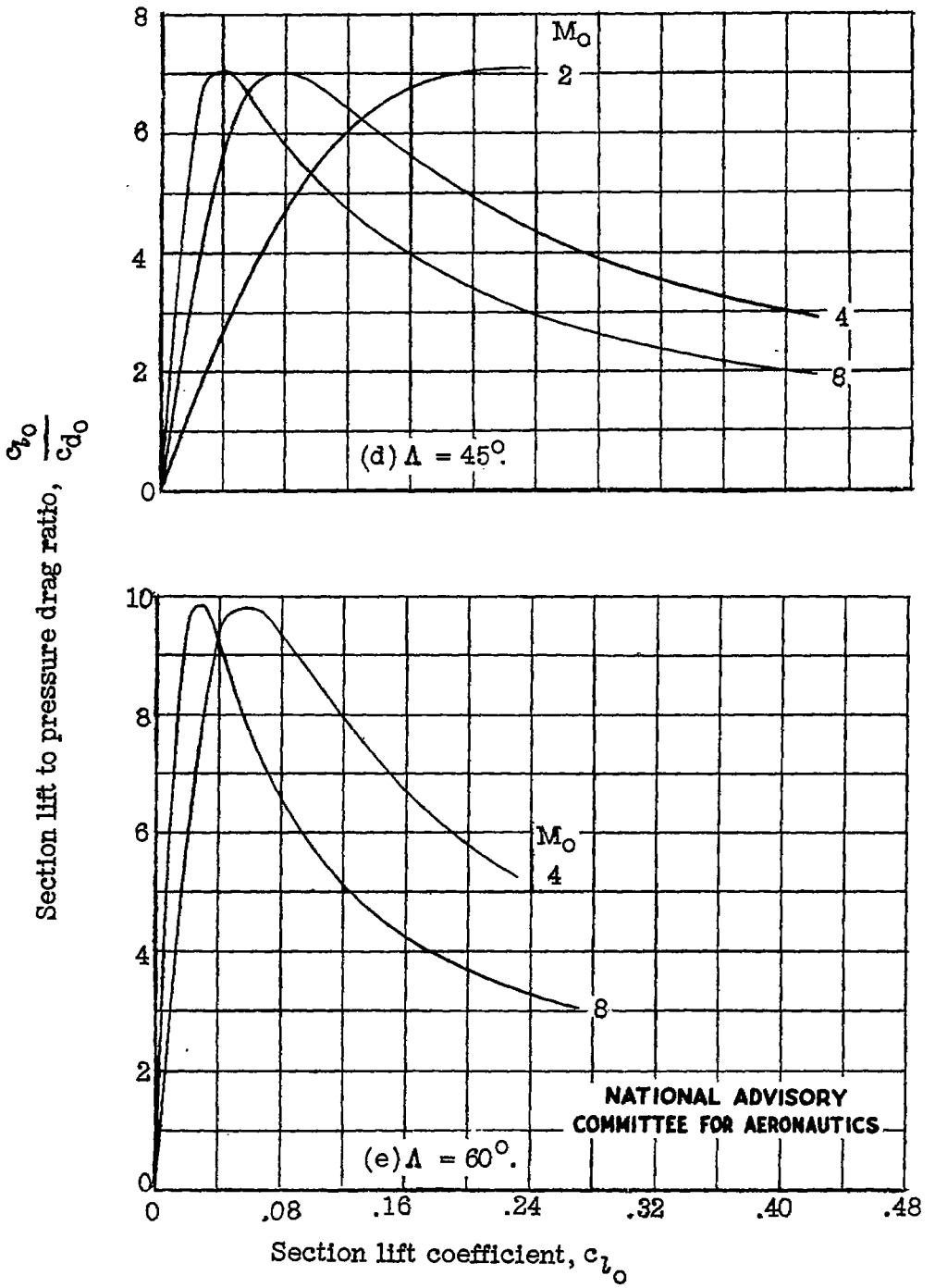

Figure 5.- Concluded.

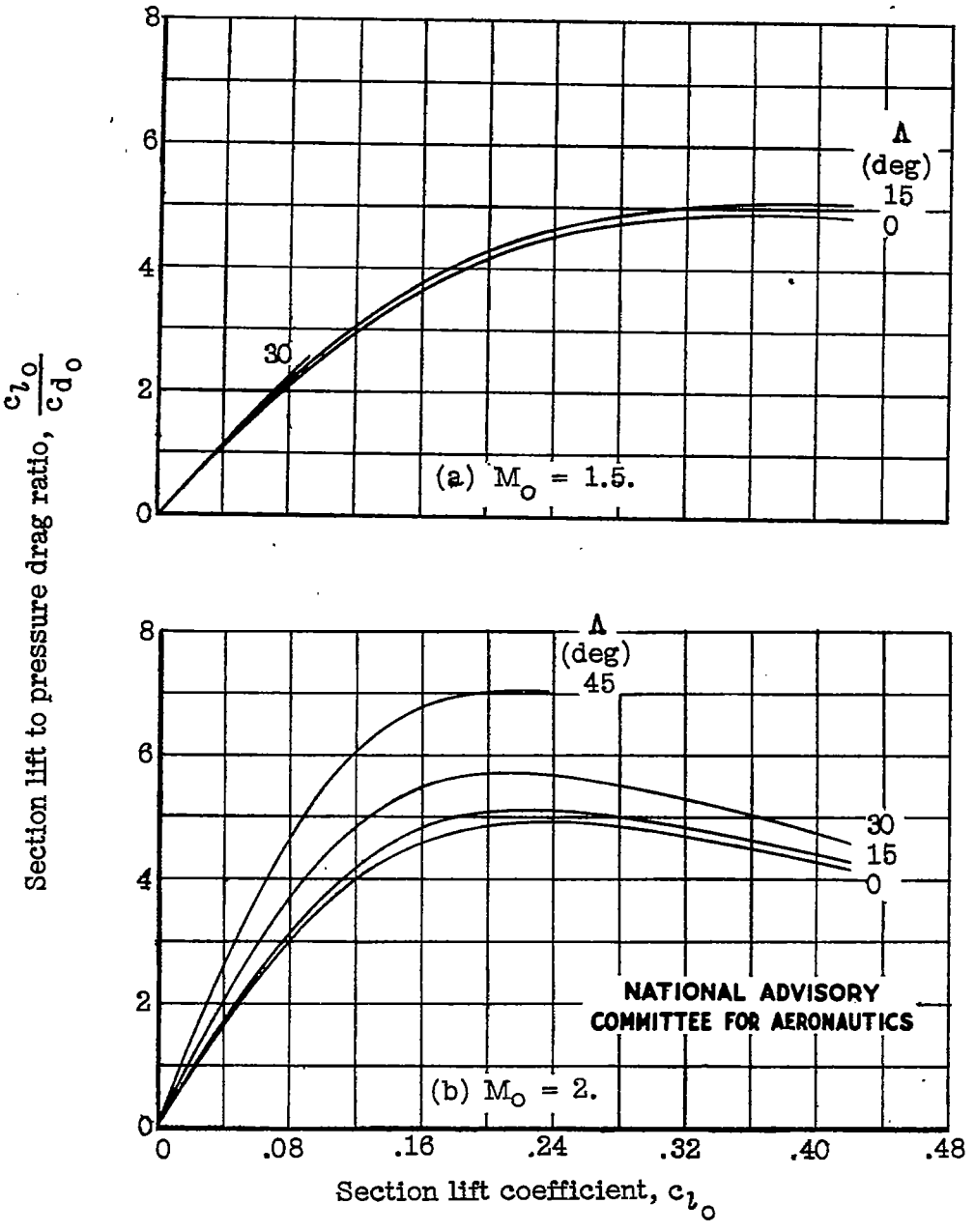

Figure 6.- Ratio of lift to pressure drag. $\left(\frac{t}{c}\right)_e = 0.10$.

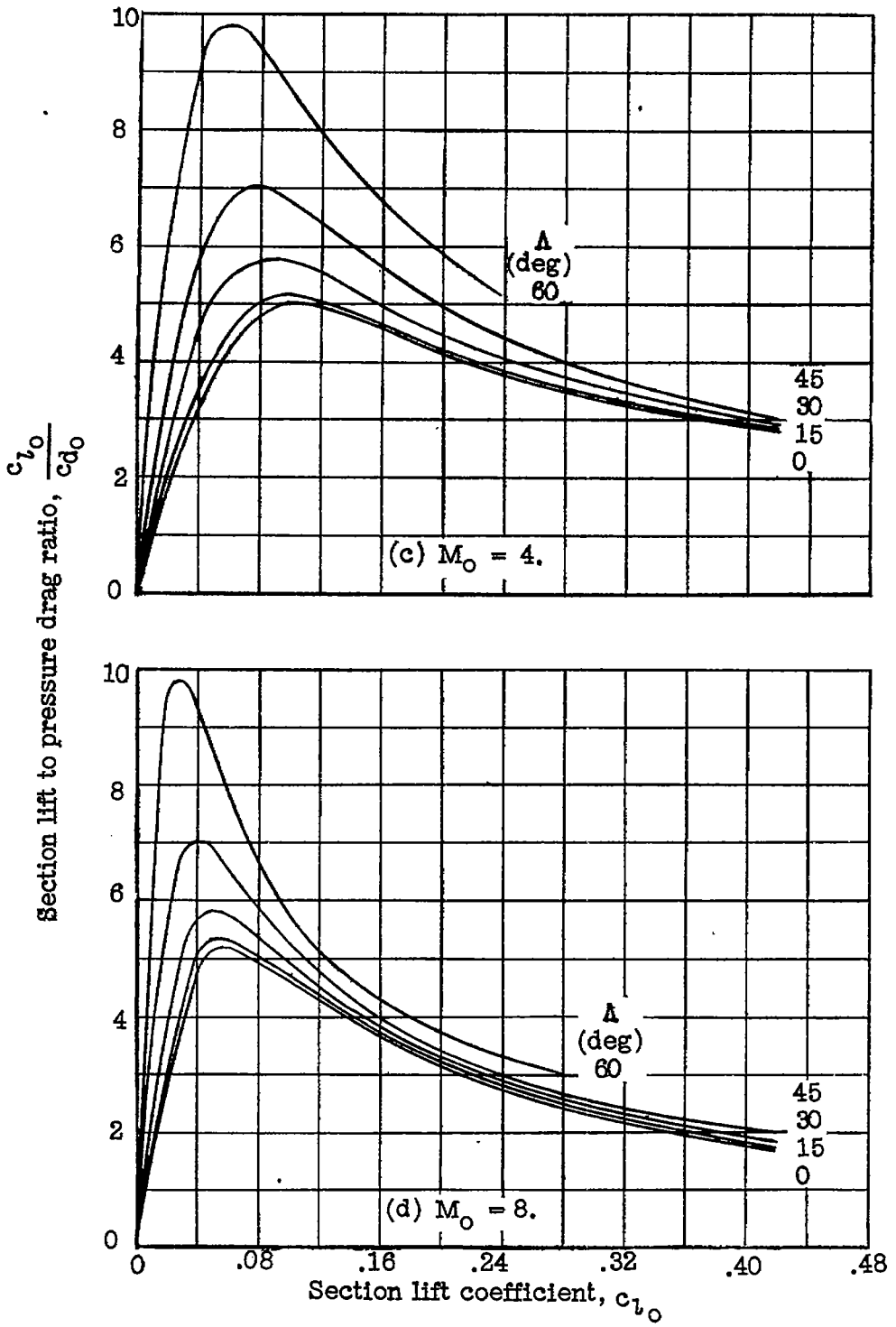

Figure 6.- Concluded.

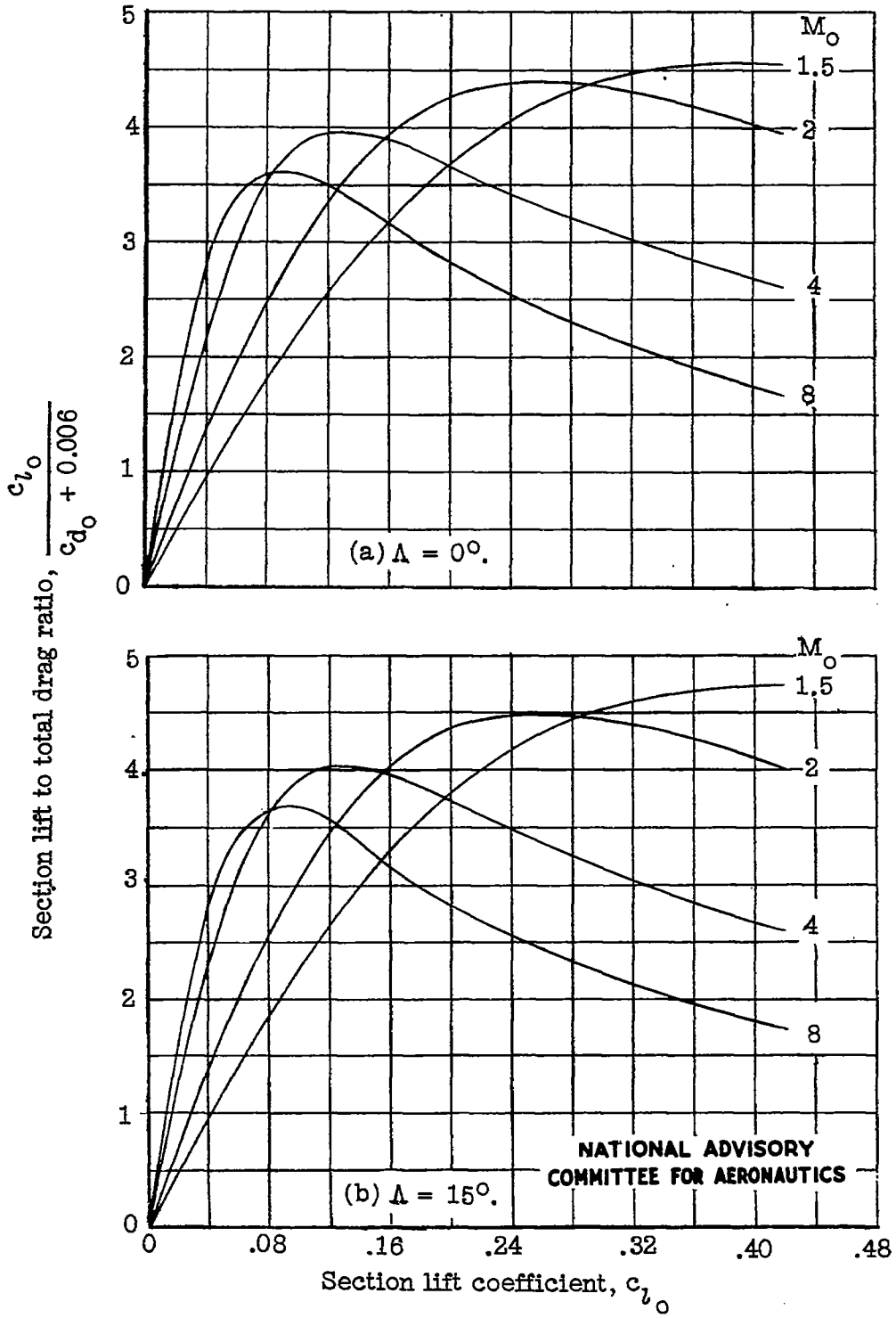

Figure 7.- Ratio of lift to total drag; $\left(\frac{t}{c}\right)_e = 0.10$.

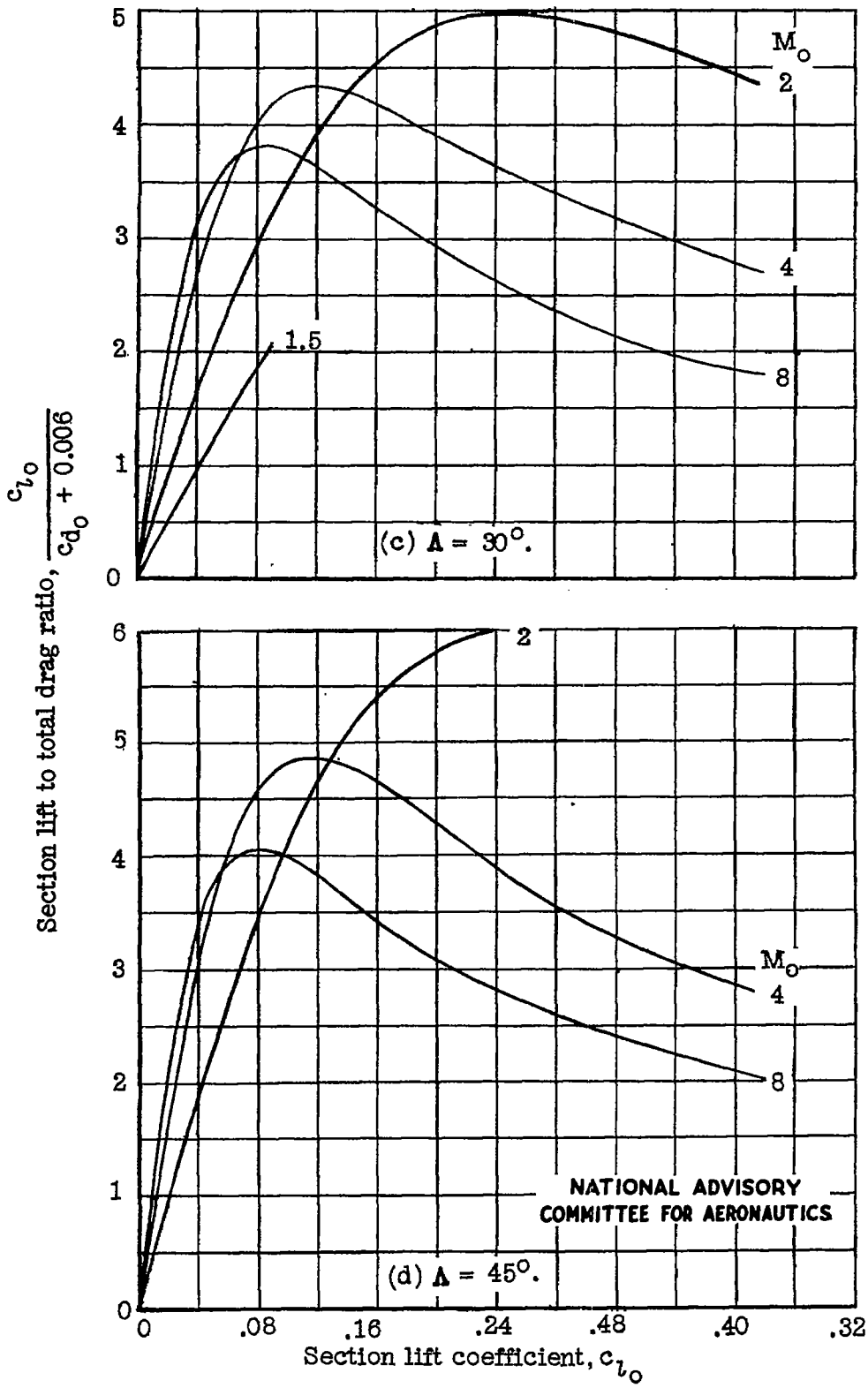

Figure 7.- Continued.

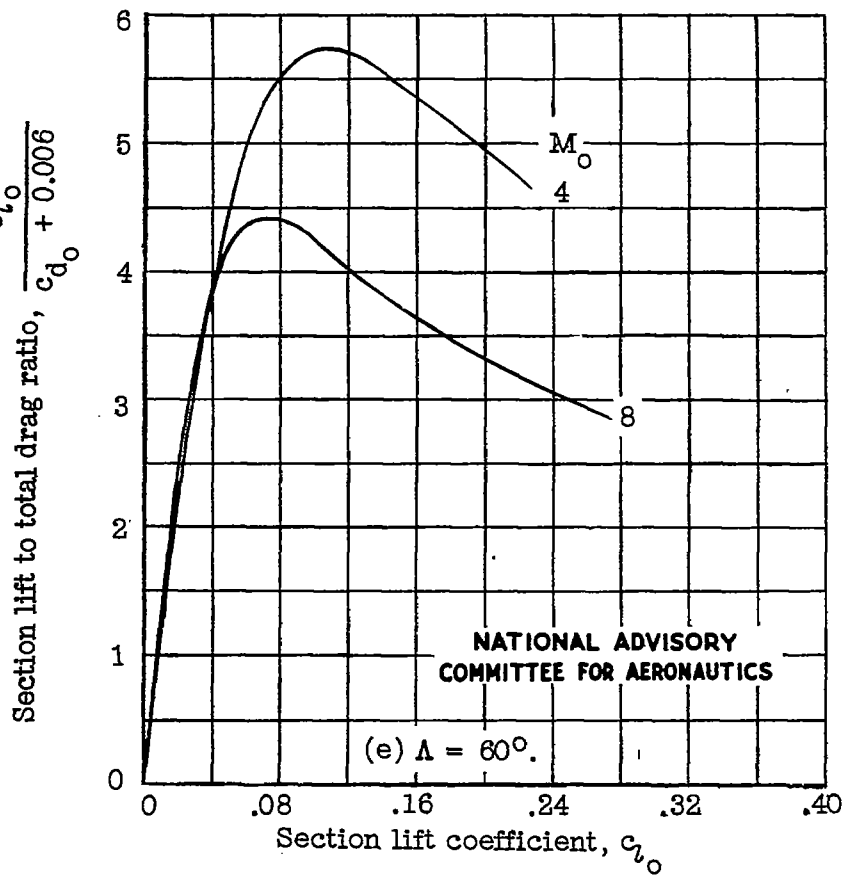

Figure 7.- Concluded.

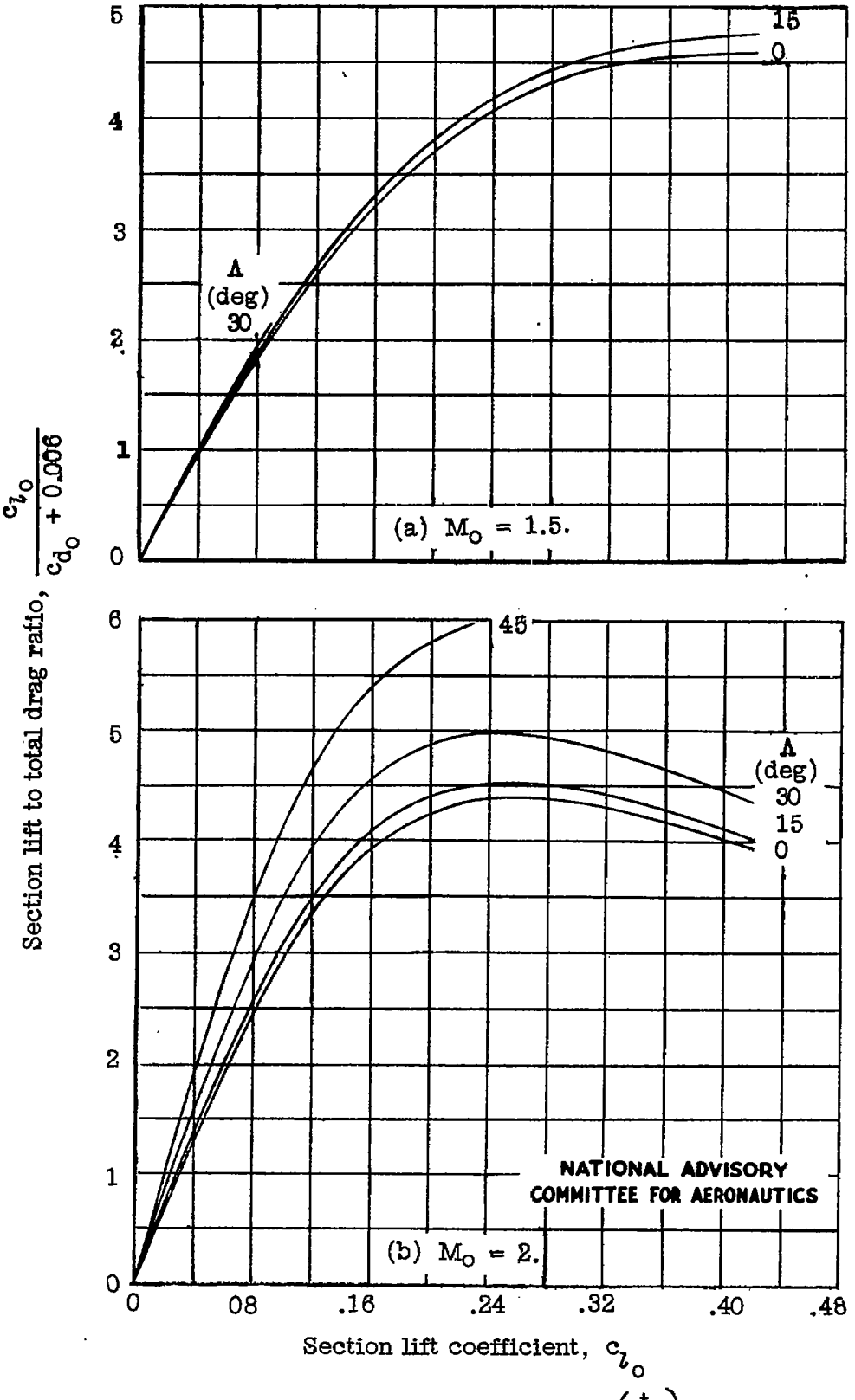

Figure 8.- Ratio of lift to total drag; $\left(\frac{t}{c}\right)_e$ = 0.10.

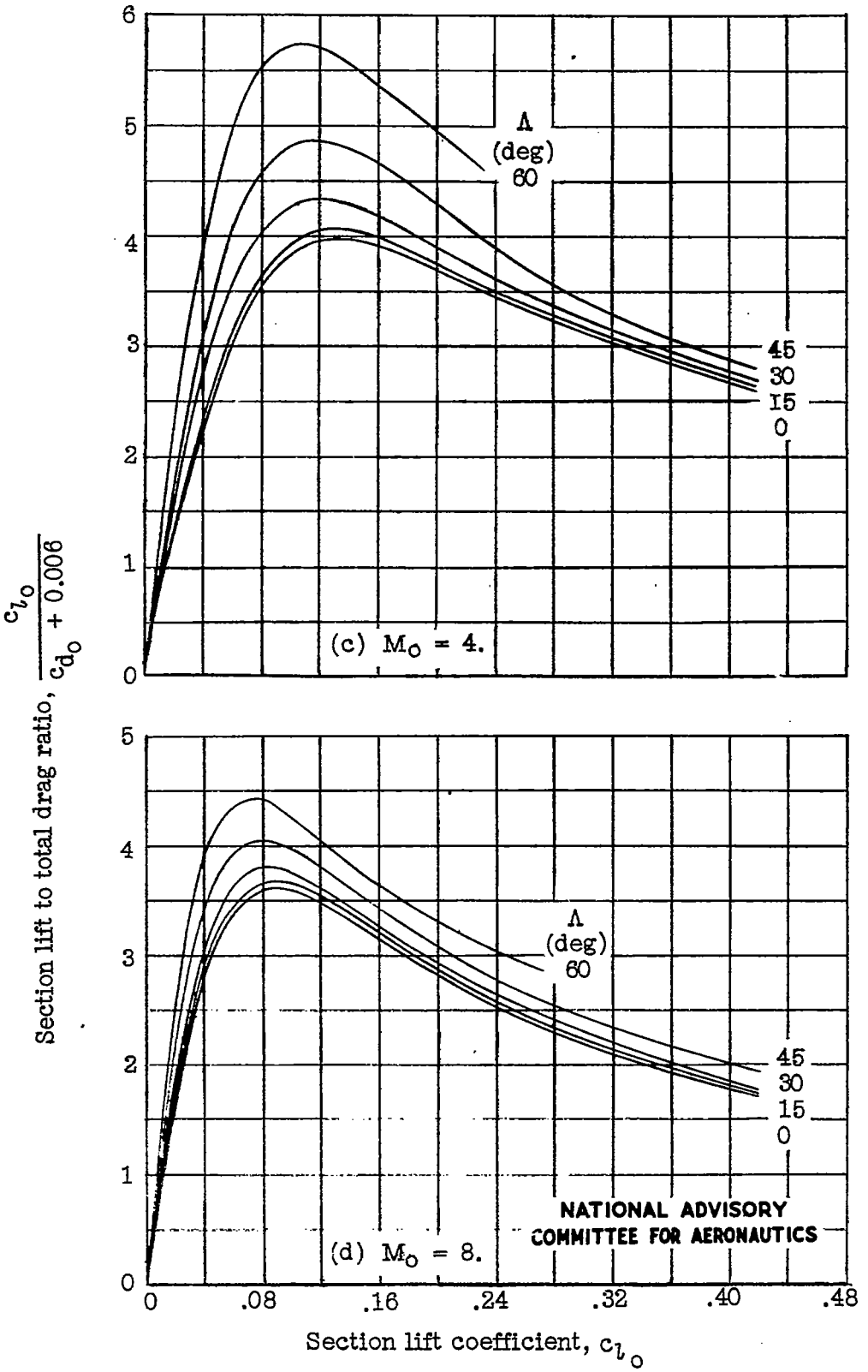

Figure 8.- Concluded.

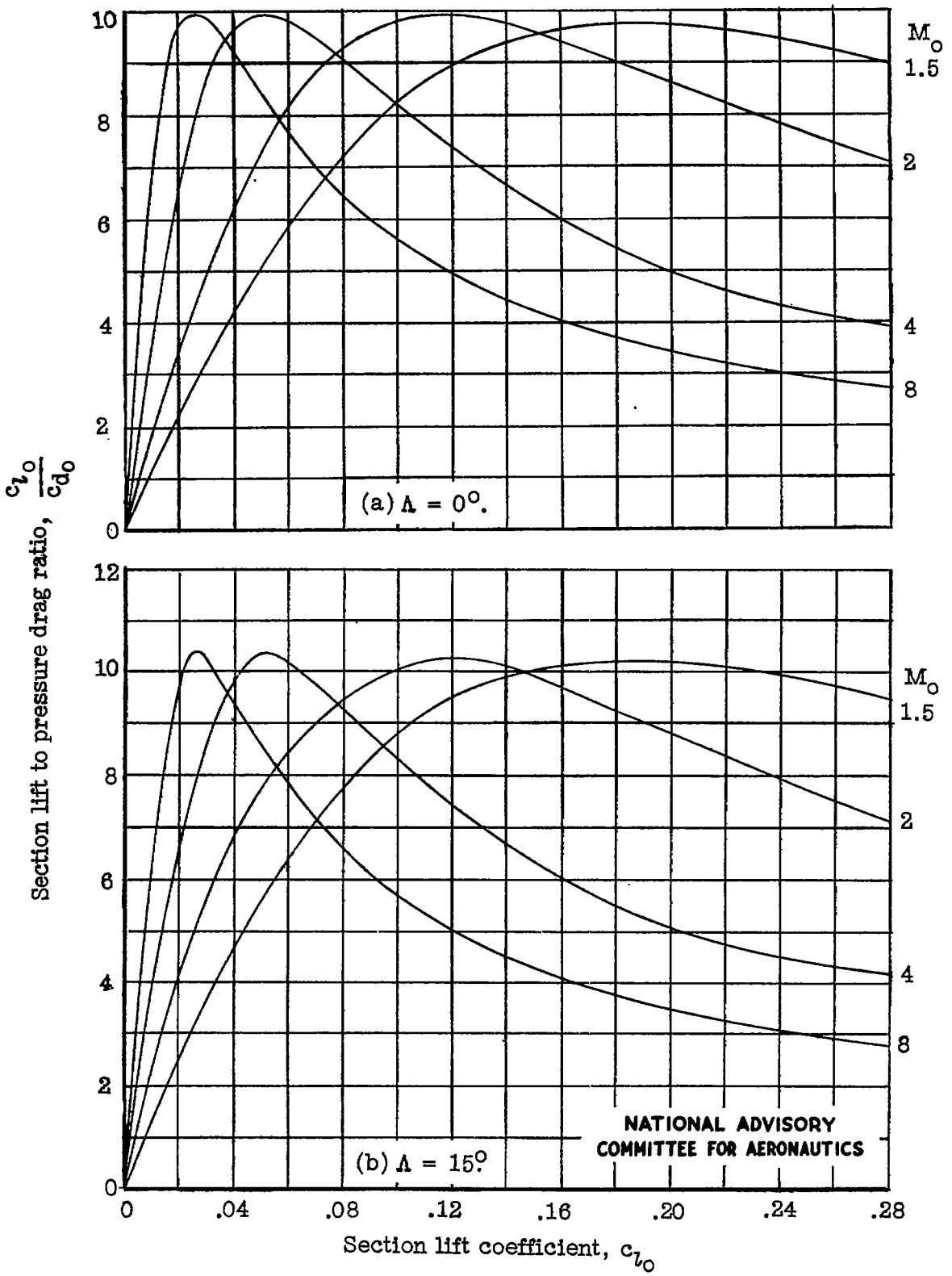

Figure 9.- Ratio of lift to pressure drag; $\left(\frac{t}{c}\right)_e = 0.05$.

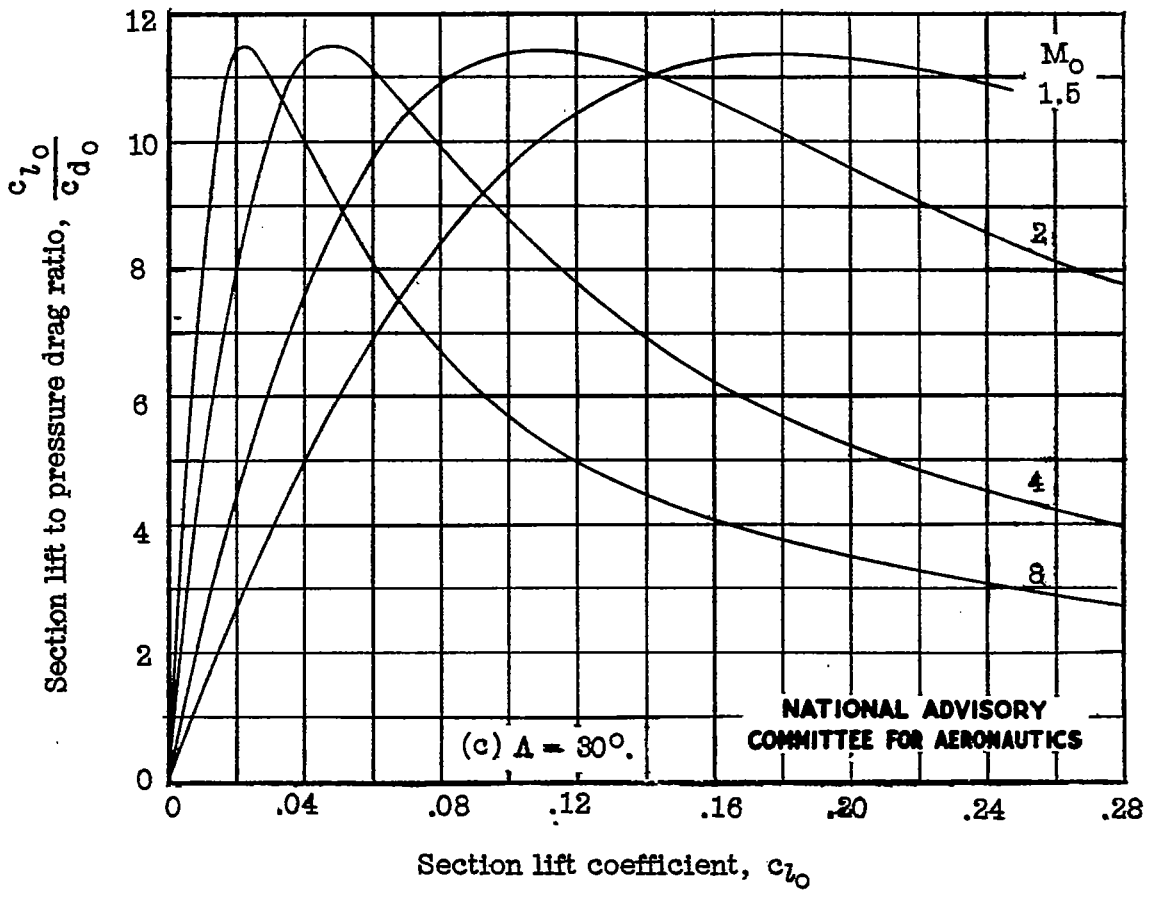

Figure 9.- Continued.

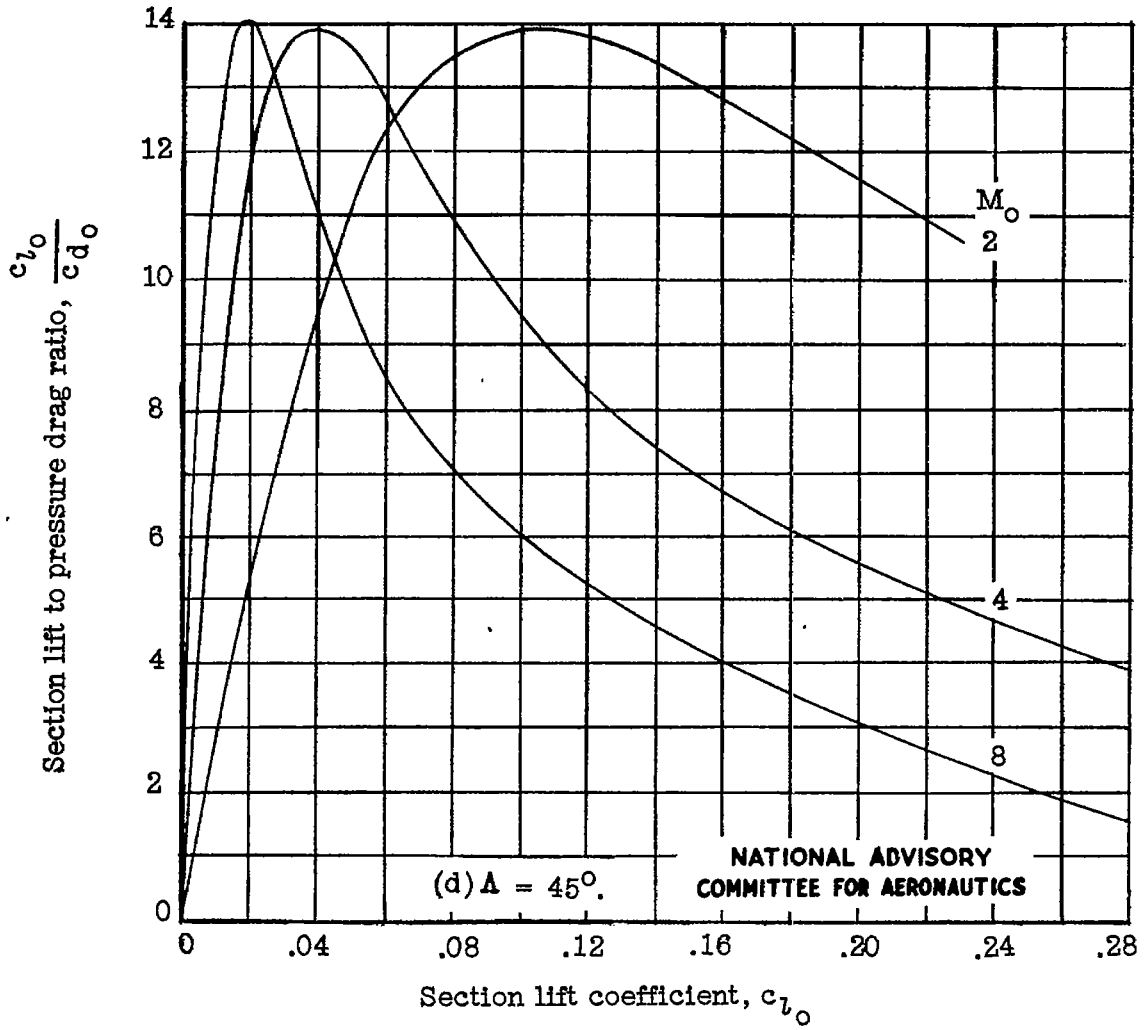

Figure 9.- Continued.

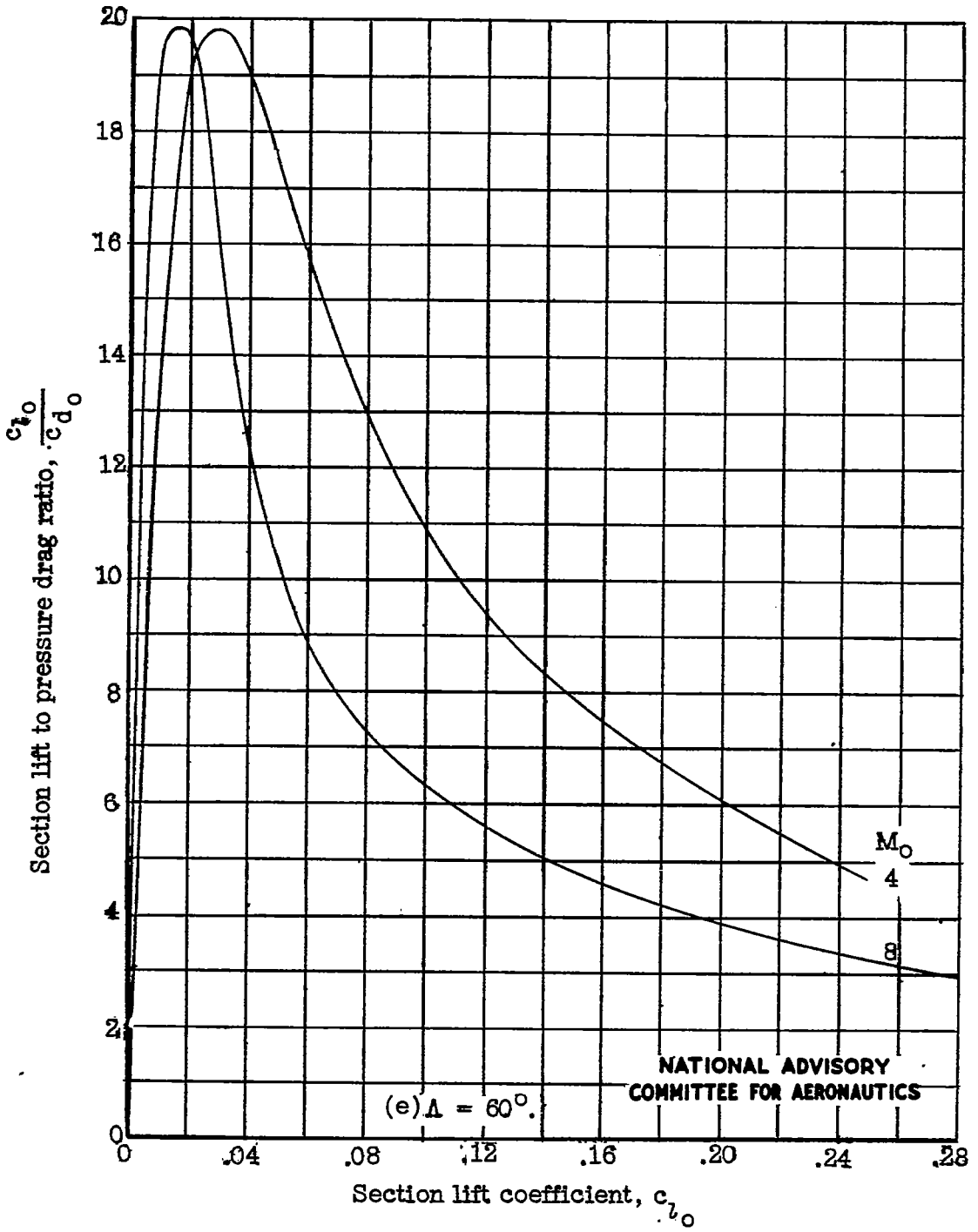

Figure 9.- Concluded.

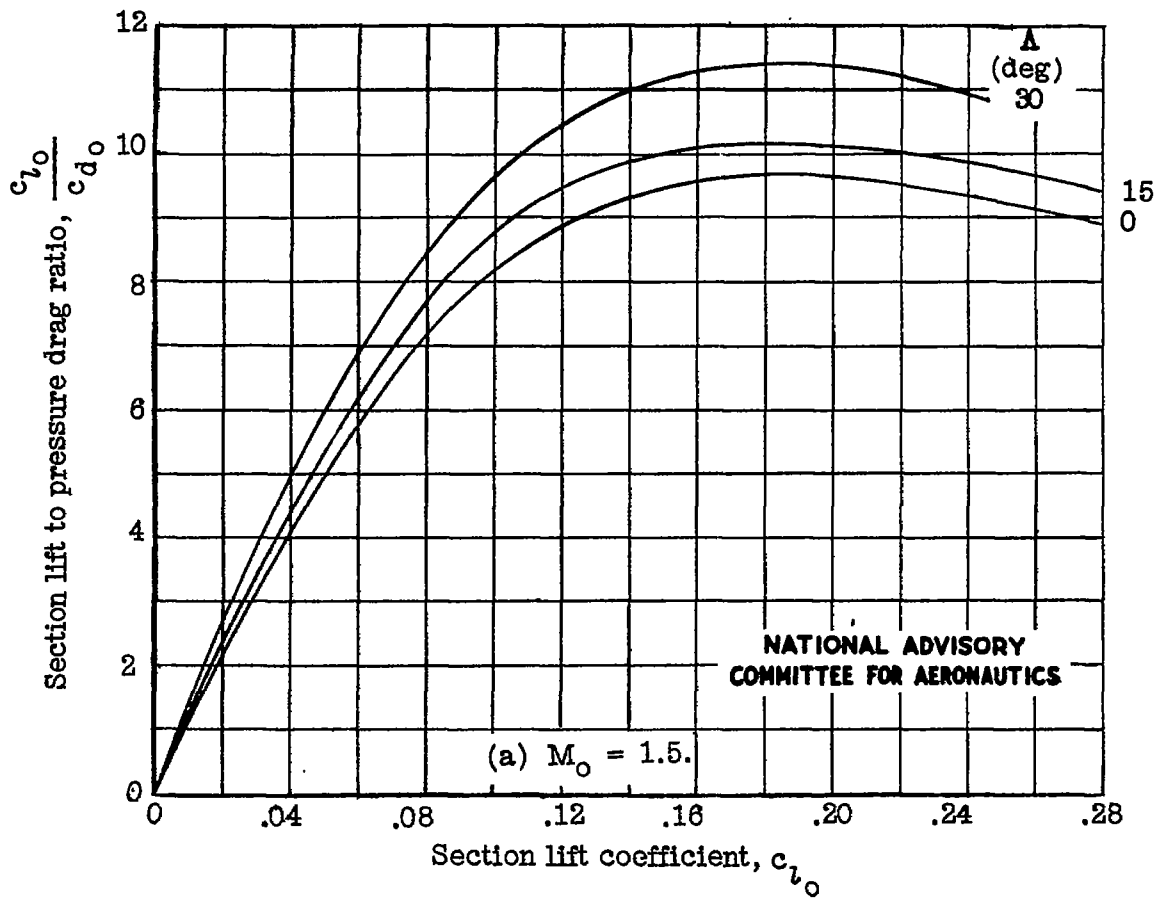

Figure 10.- Ratio of lift to pressure drag; $\left(\frac{t}{c}\right)_e$ = 0.05.

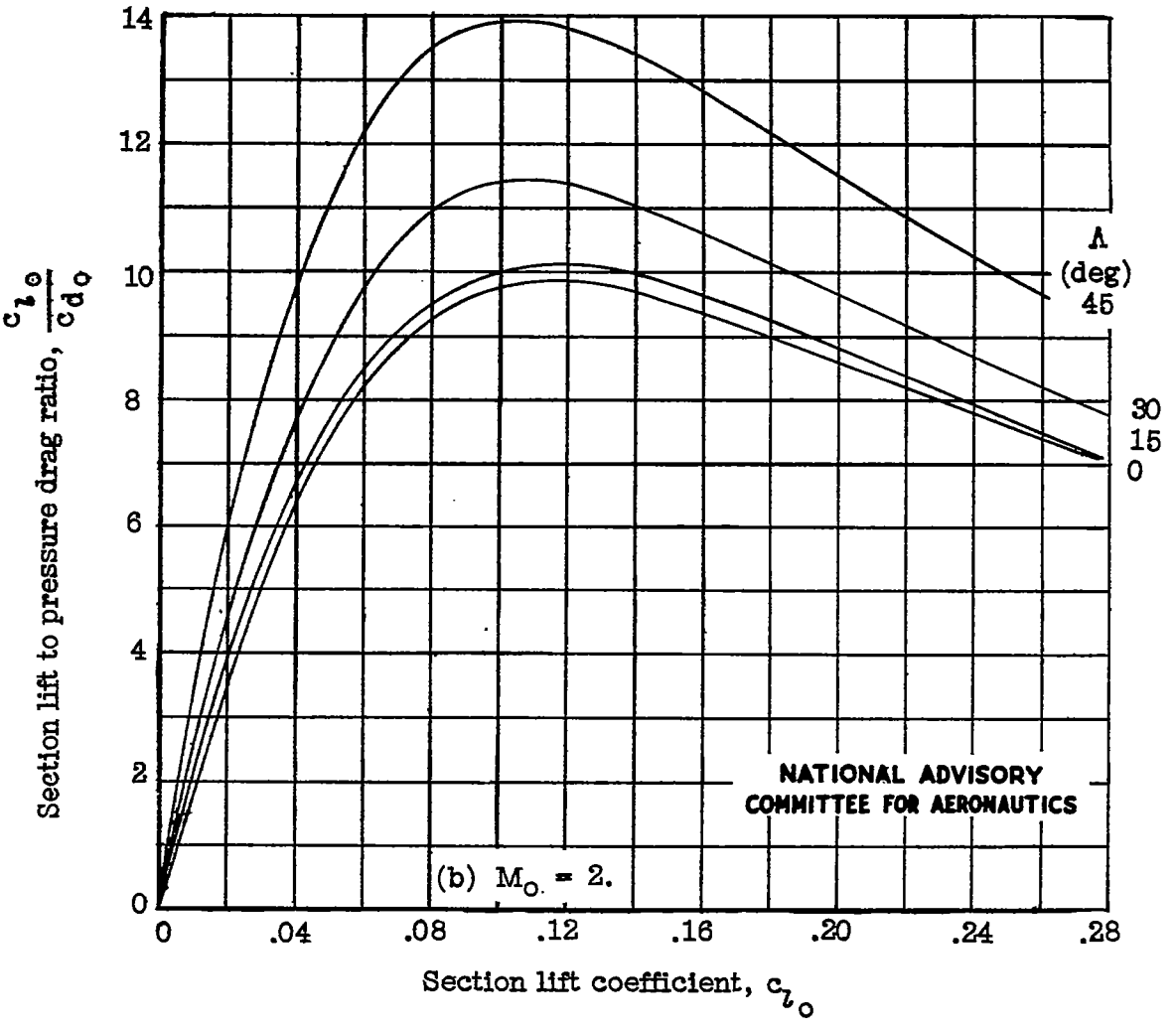

Figure 10.- Continued.

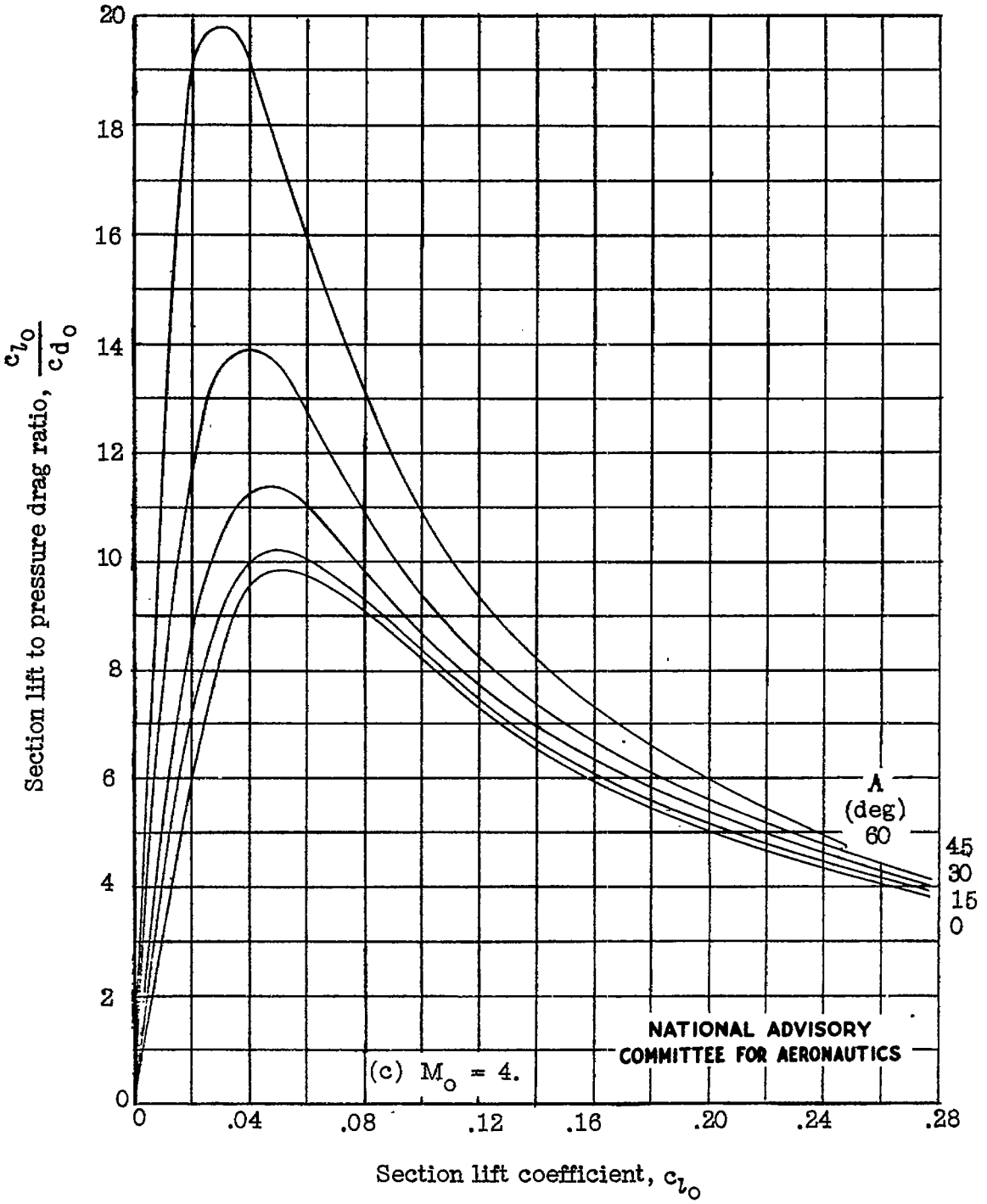

Figure 10.- Continued.

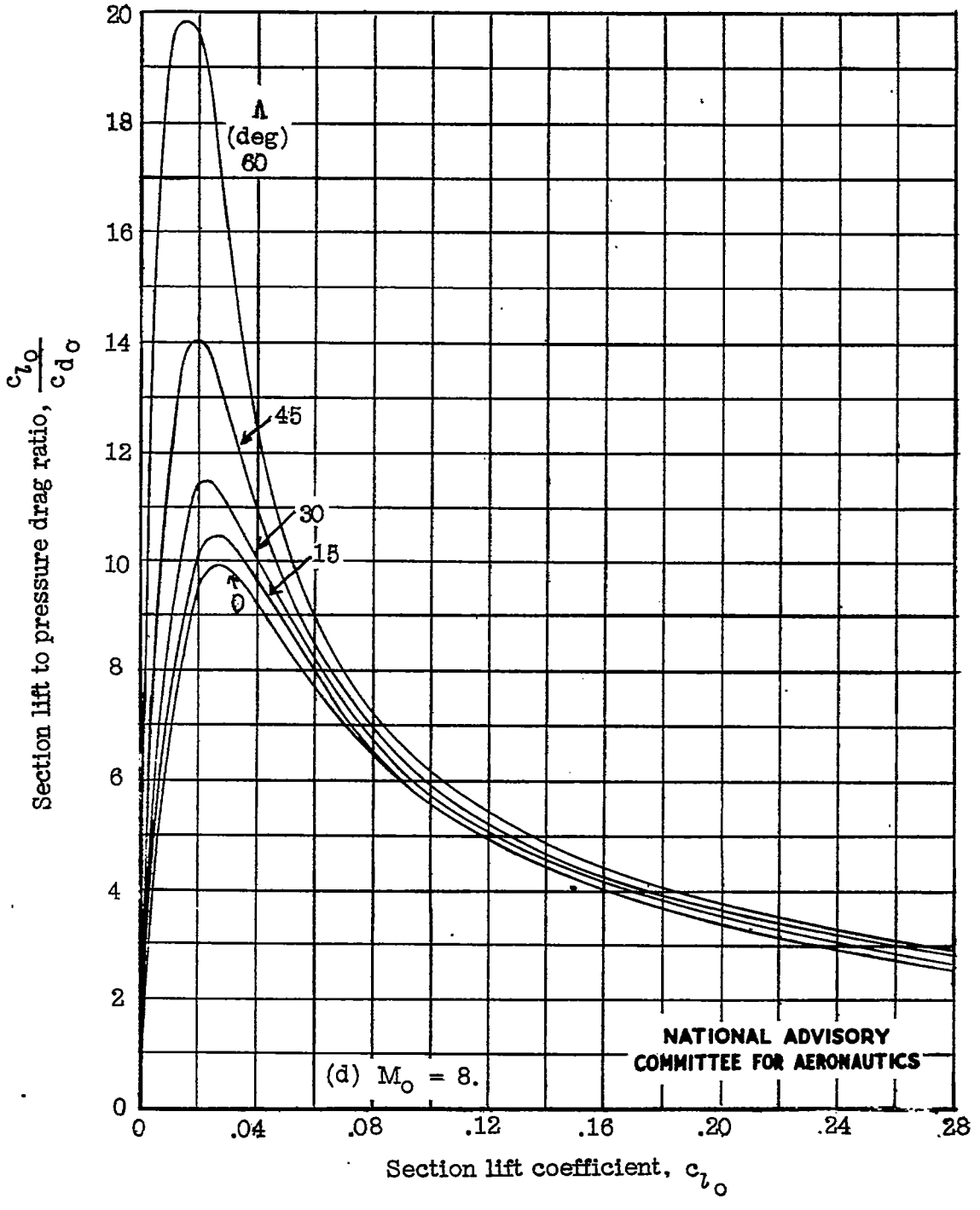

Figure 10.- Concluded.

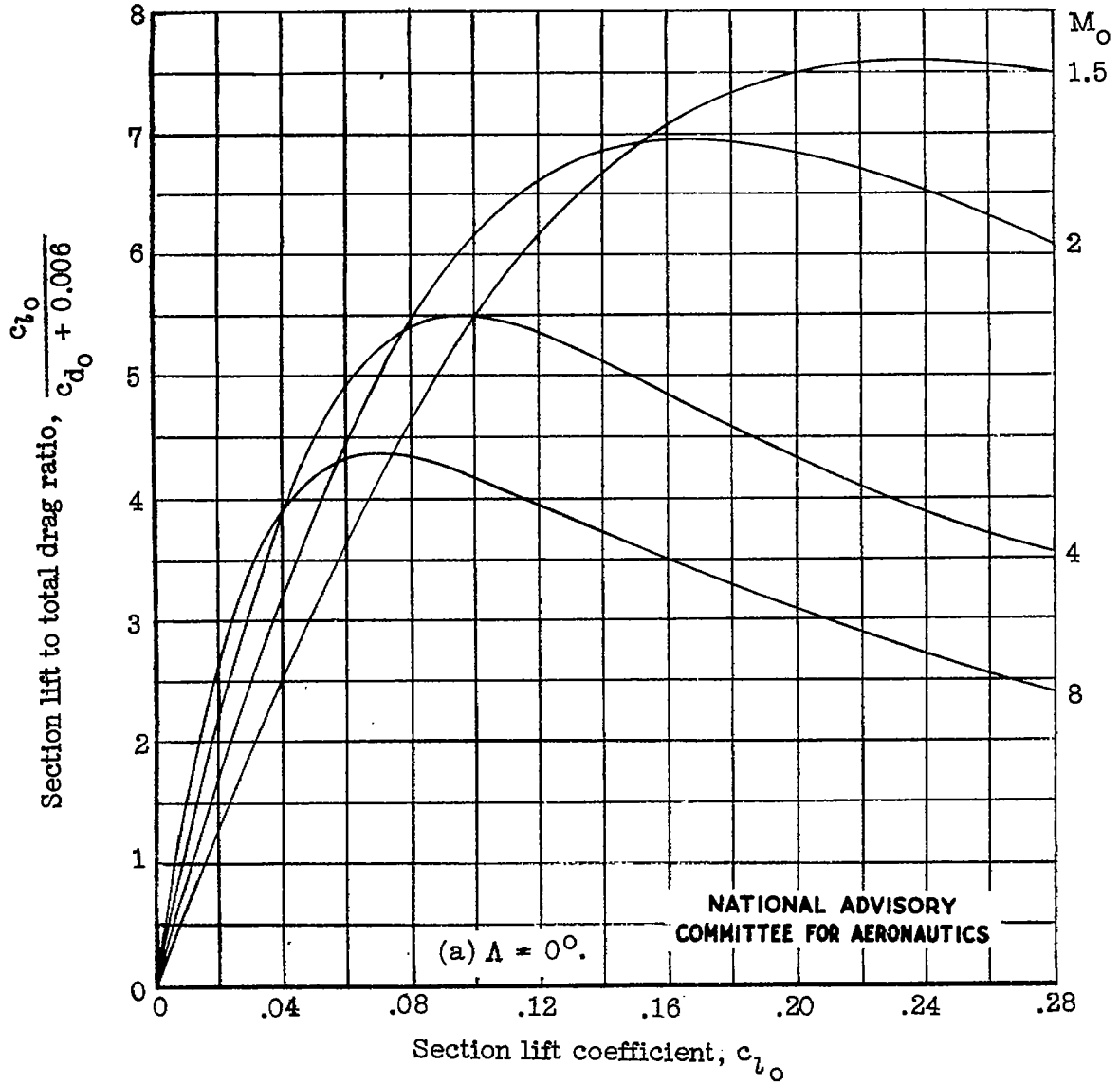

Figure 11.- Ratio of lift to total drag; $\left(\frac{t}{c}\right)_e = 0.05$.

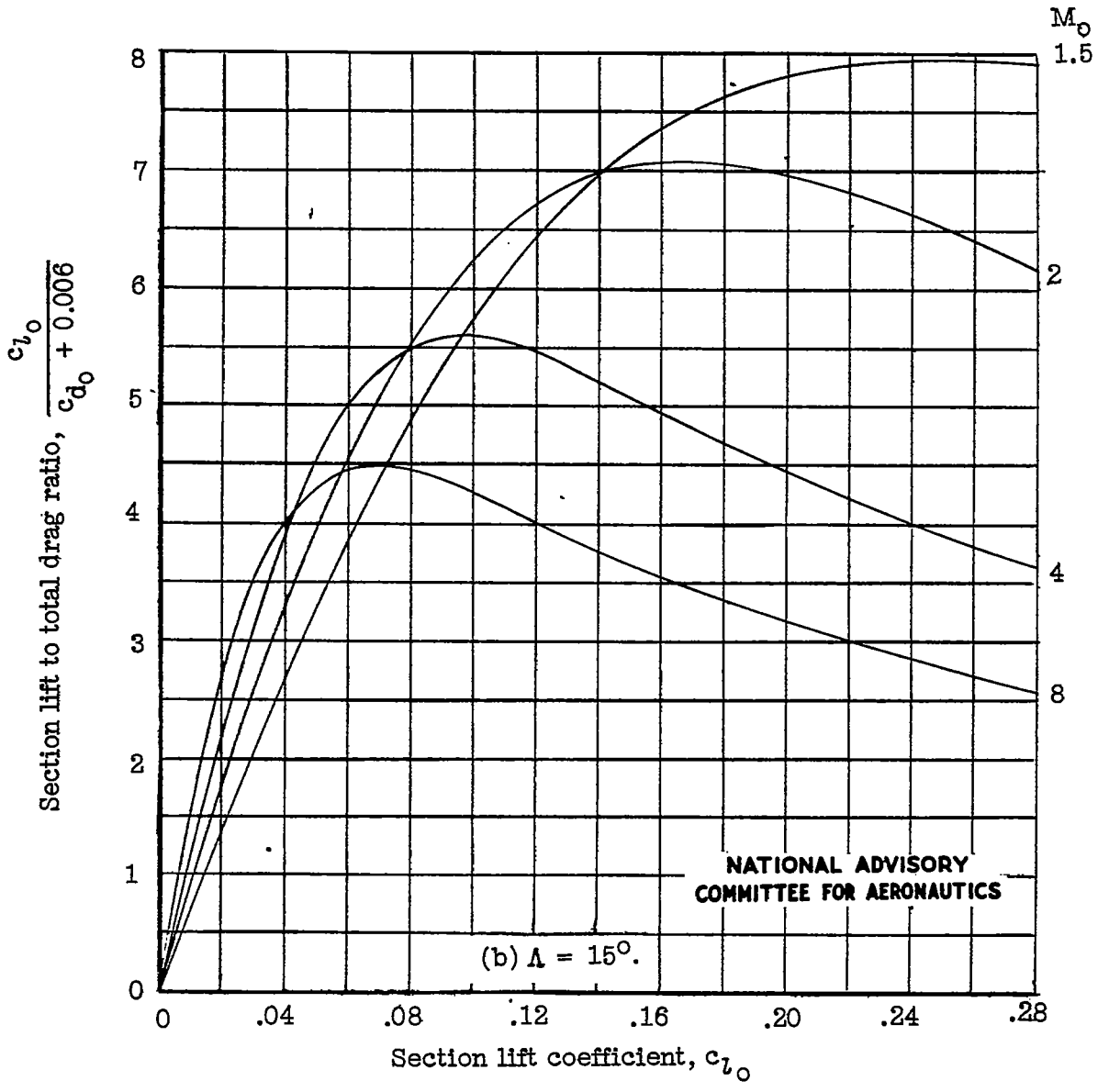

Figure 11.- Continued.

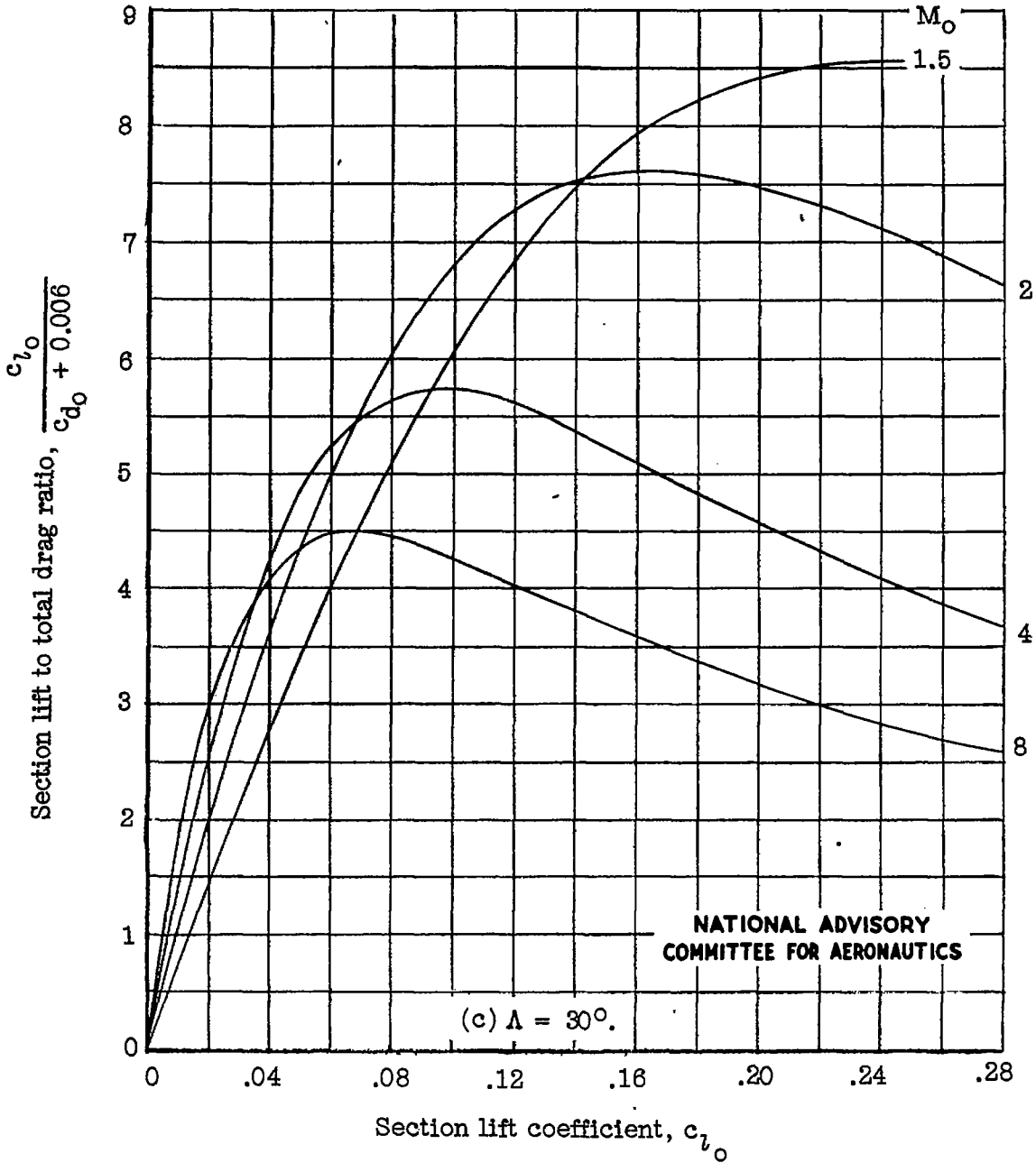

Figure 11.- Continued.

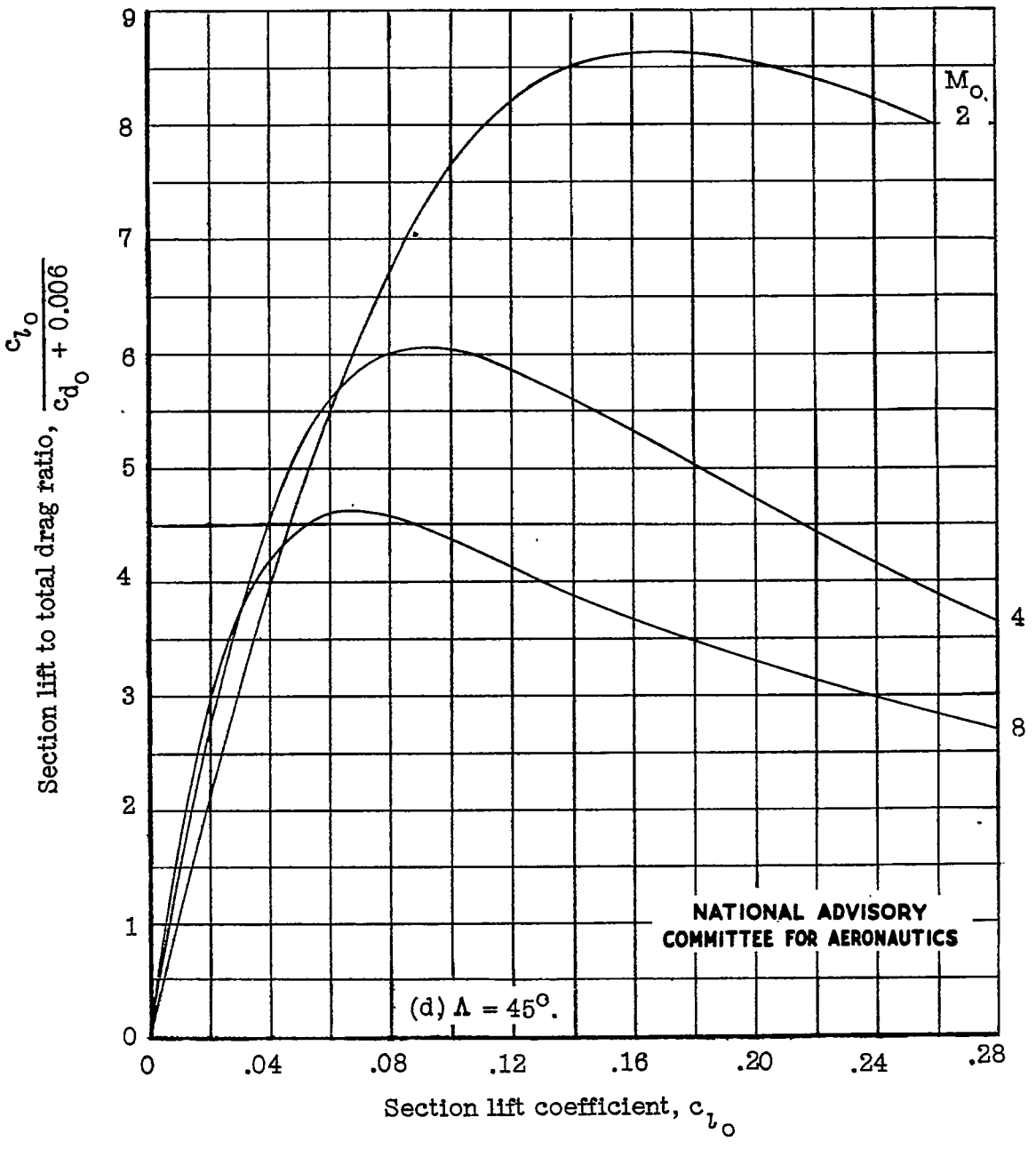

Figure 11.- Continued.

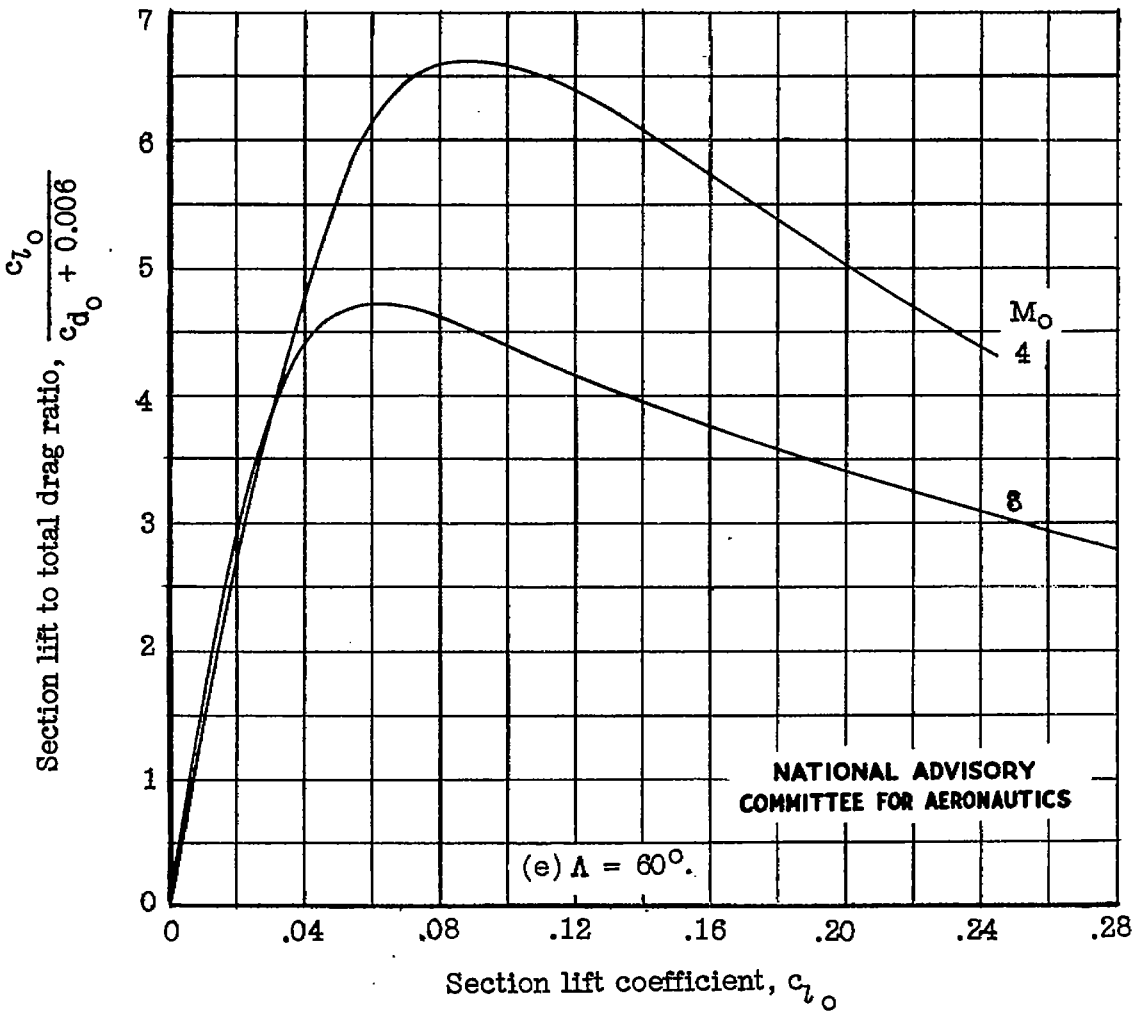

Figure 11.- Concluded.

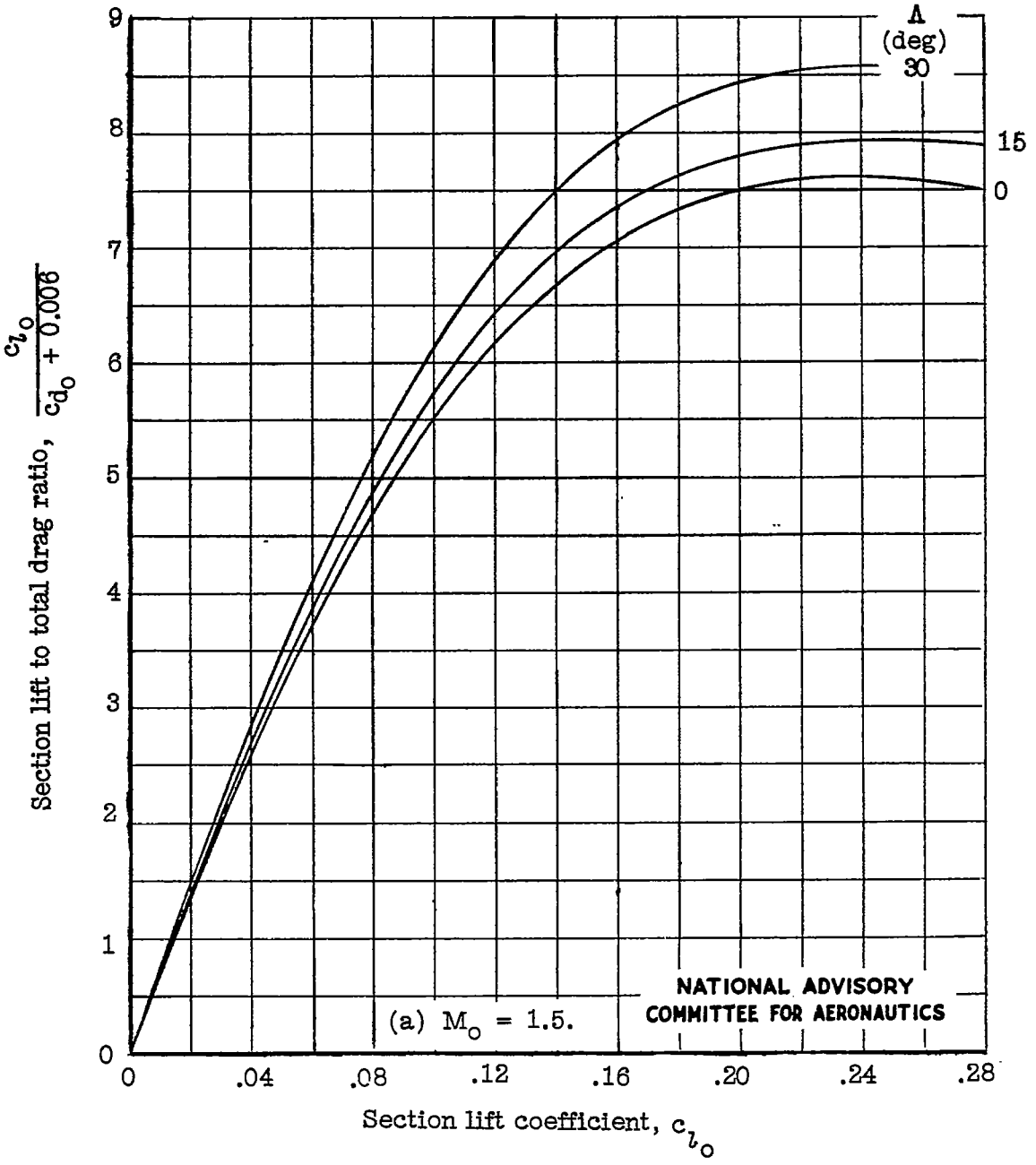

Figure 12.- Ratio of lift to total drag; $\left(\frac{t}{c}\right)_e = 0.05$.

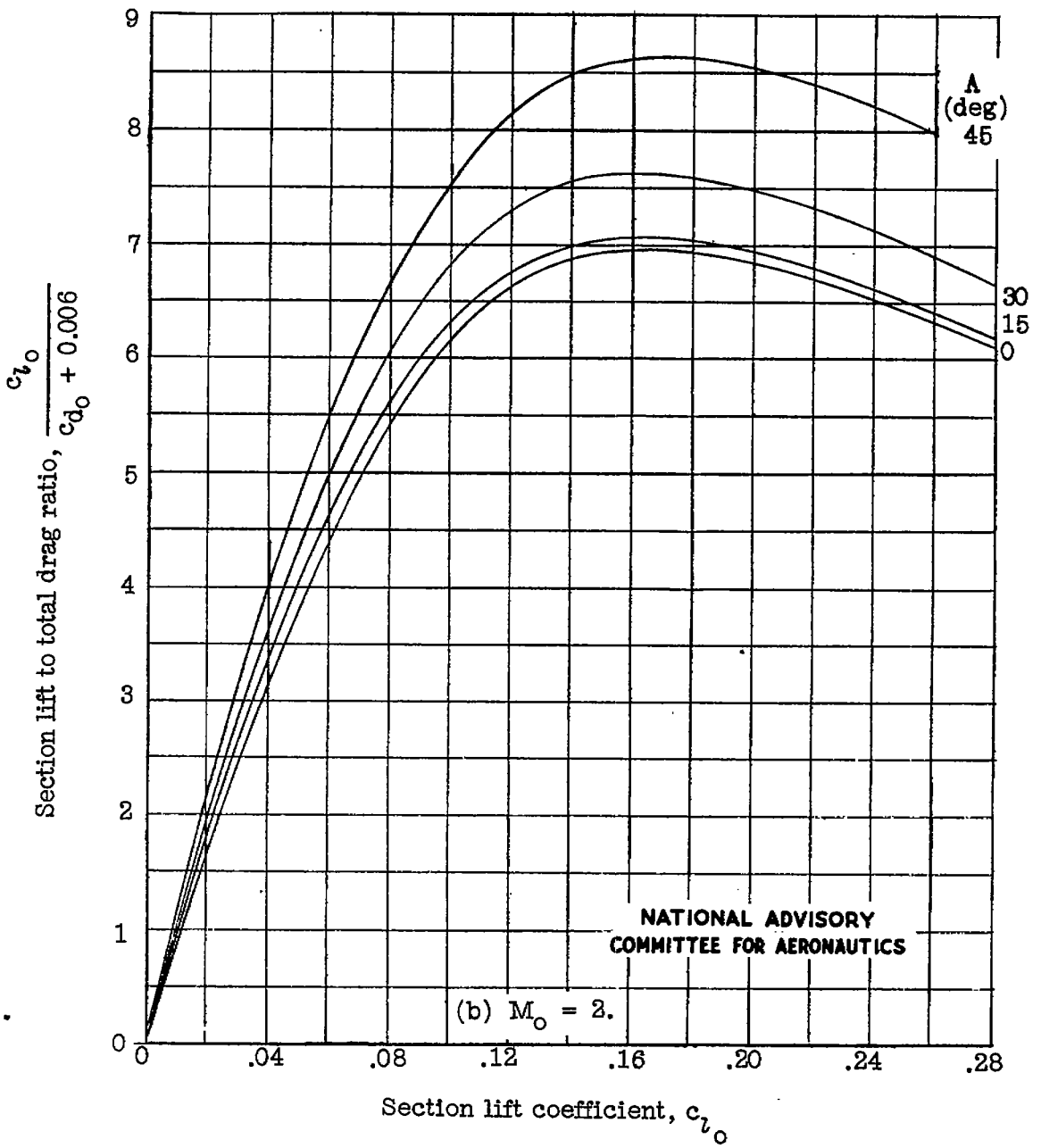

Figure 12.- Continued.

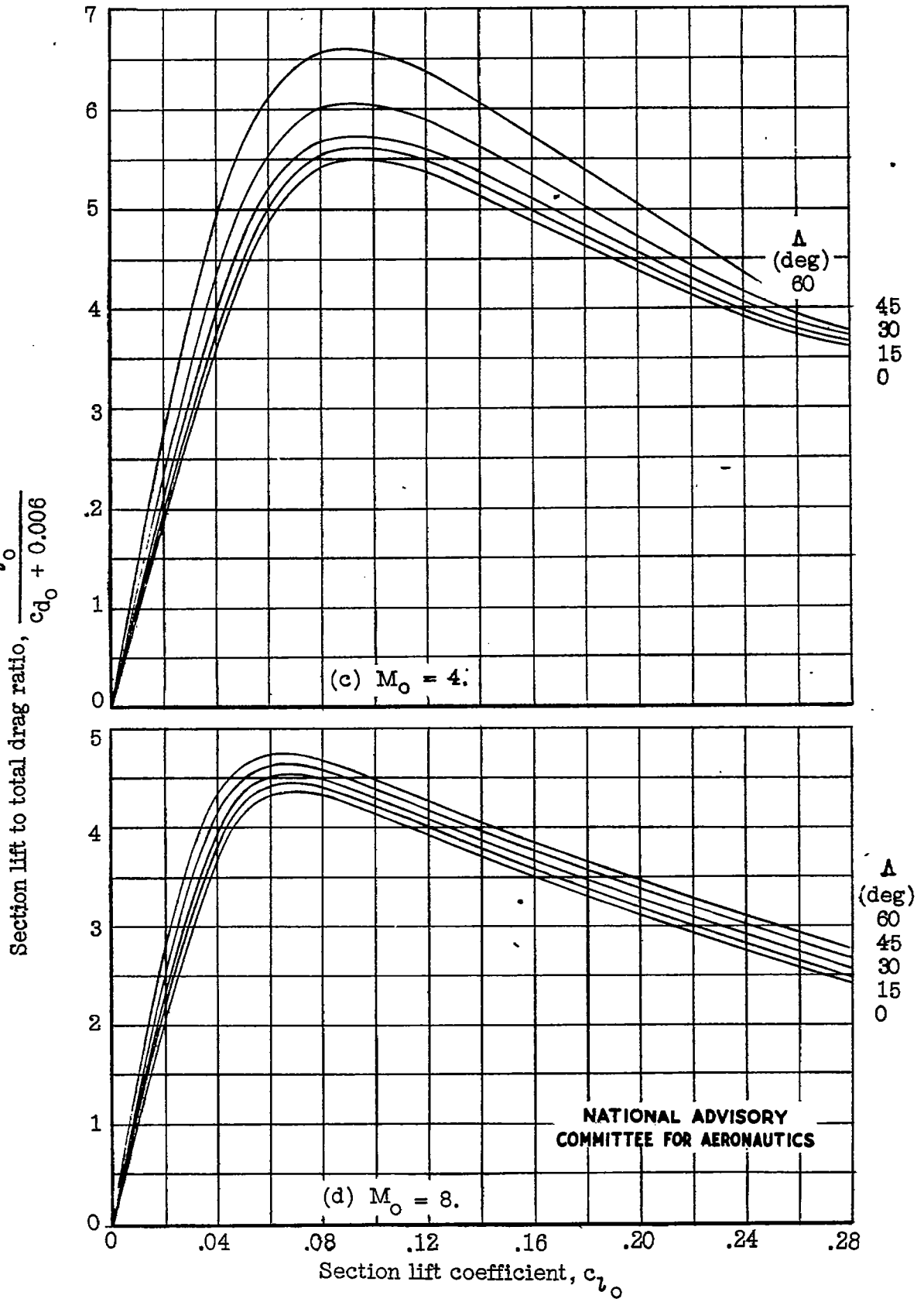

Figure 12.- Concluded.

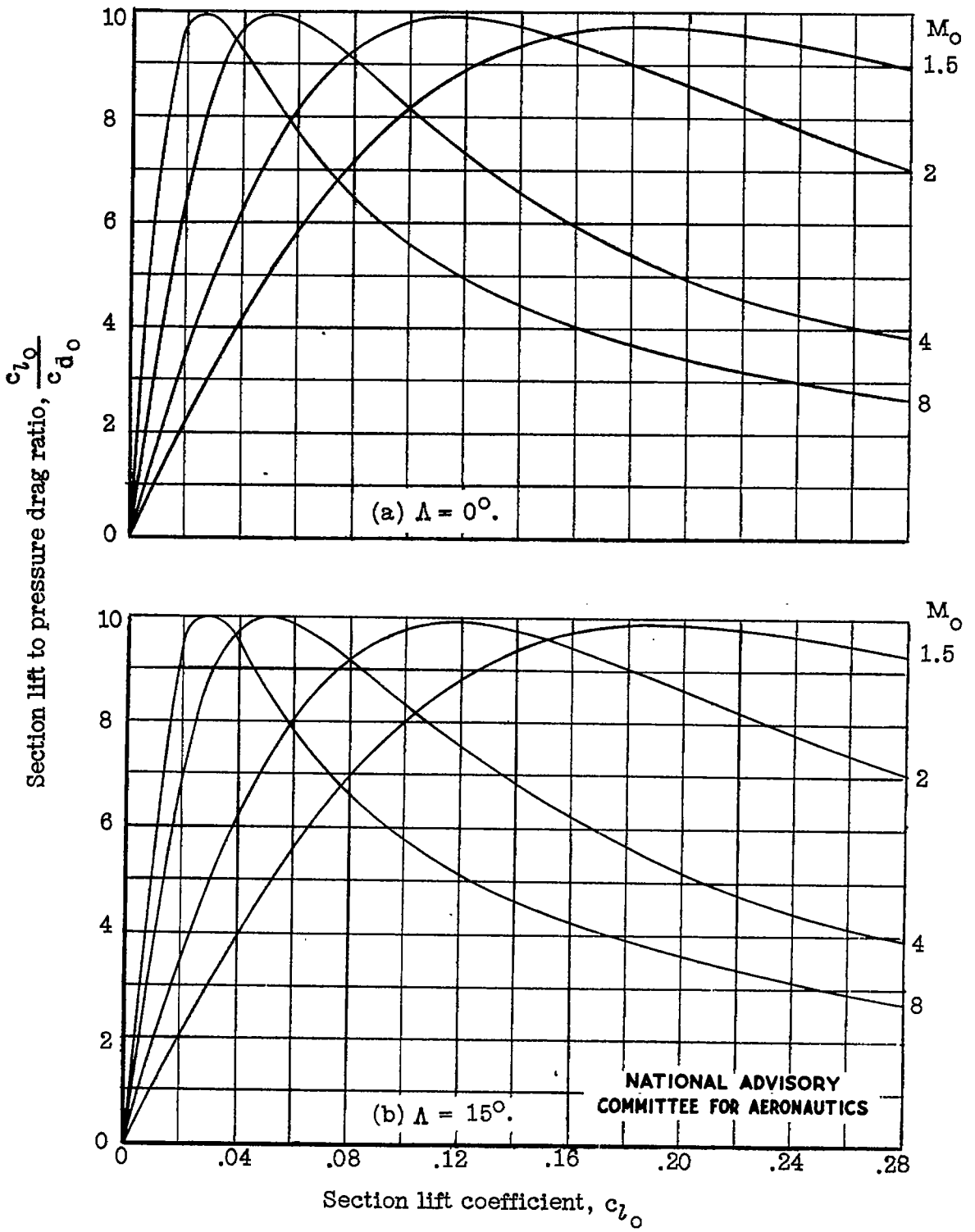

Figure 13.- Ratio of lift to pressure drag; $\left(\frac{t}{c}\right)_o = 0.05$.

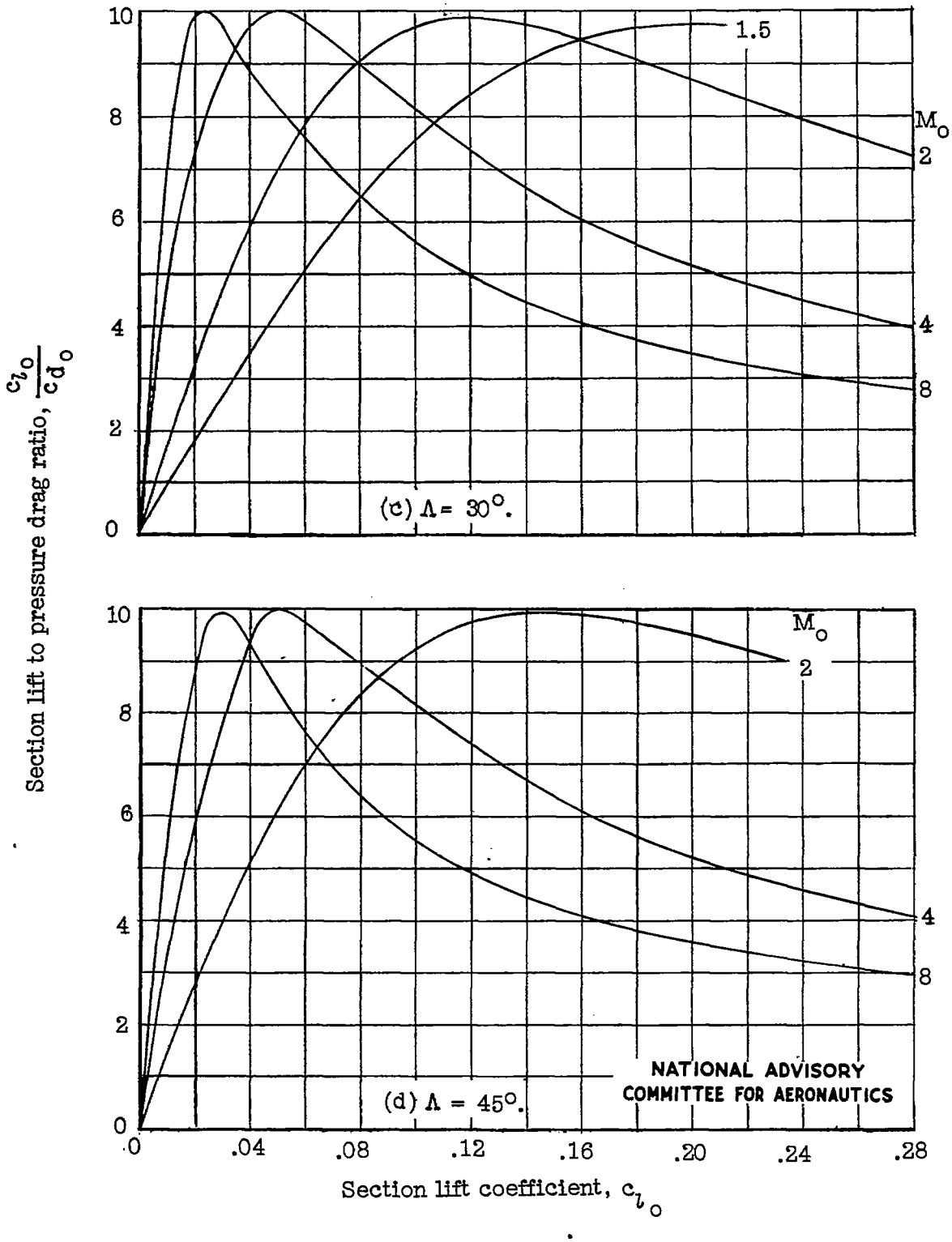

Figure 13.- Continued.

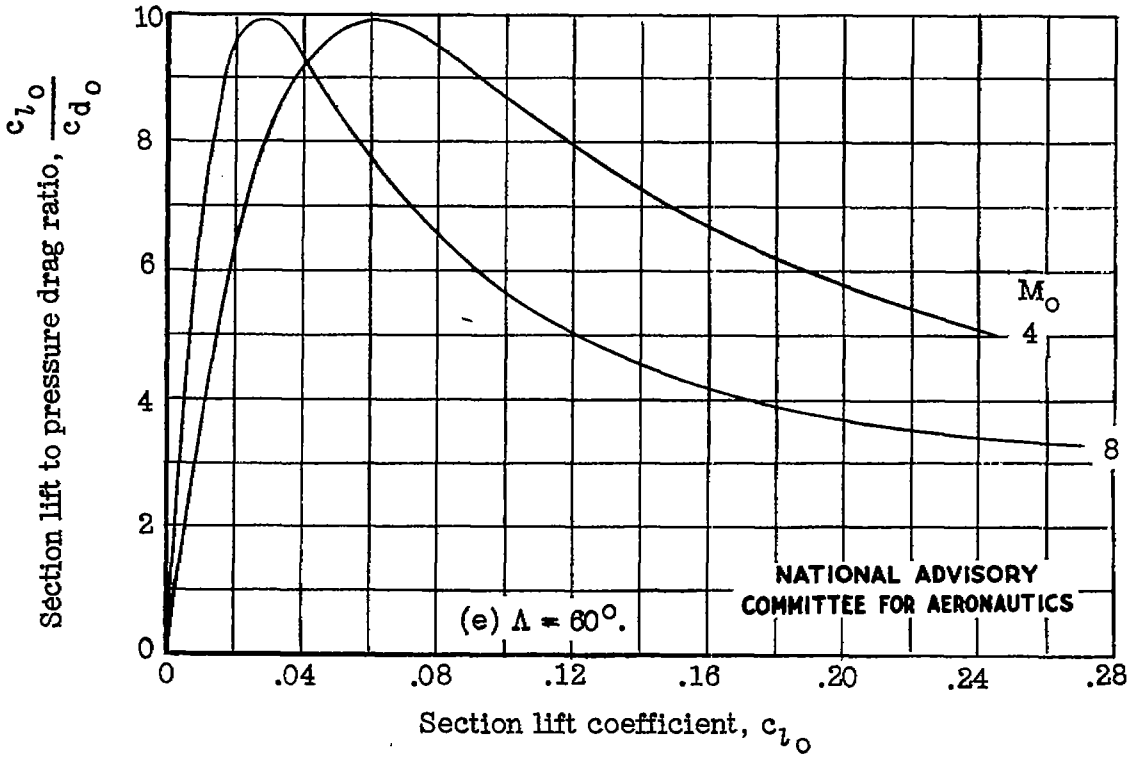

Figure 13.- Concluded.

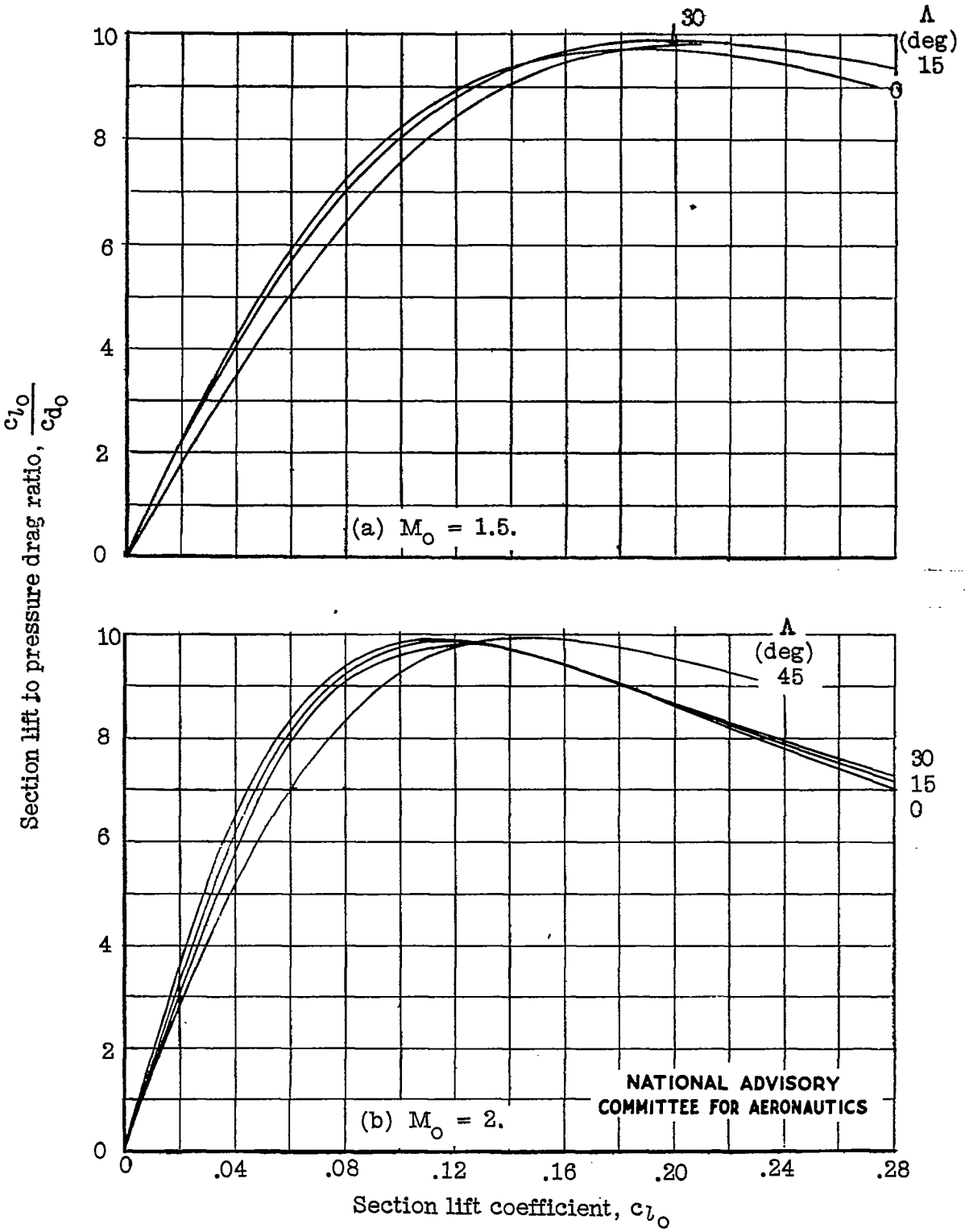

Figure 14.- Ratio of lift to pressure drag; $\left(\frac{t}{c}\right)_o = 0.05$.

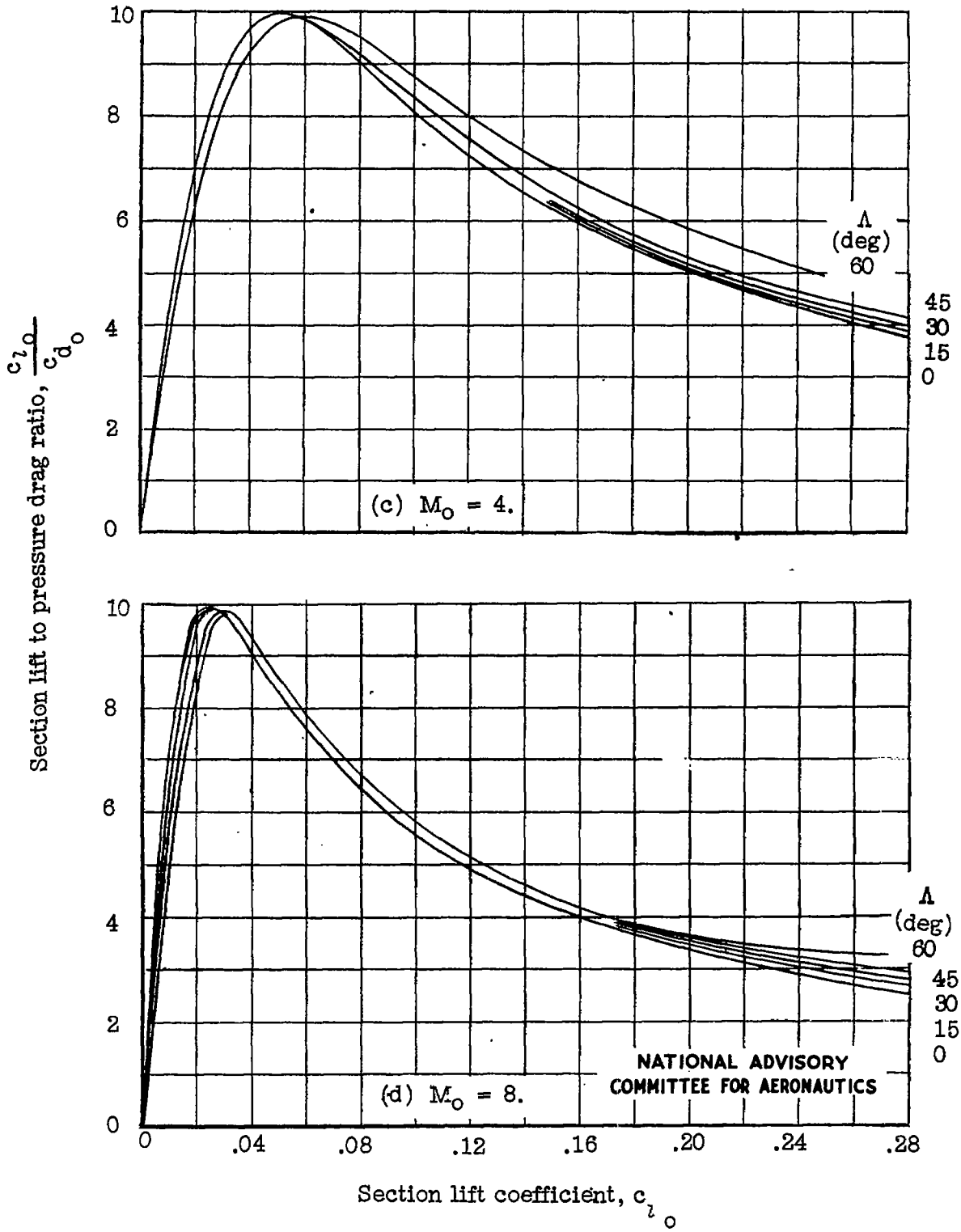

Figure 14.- Concluded.

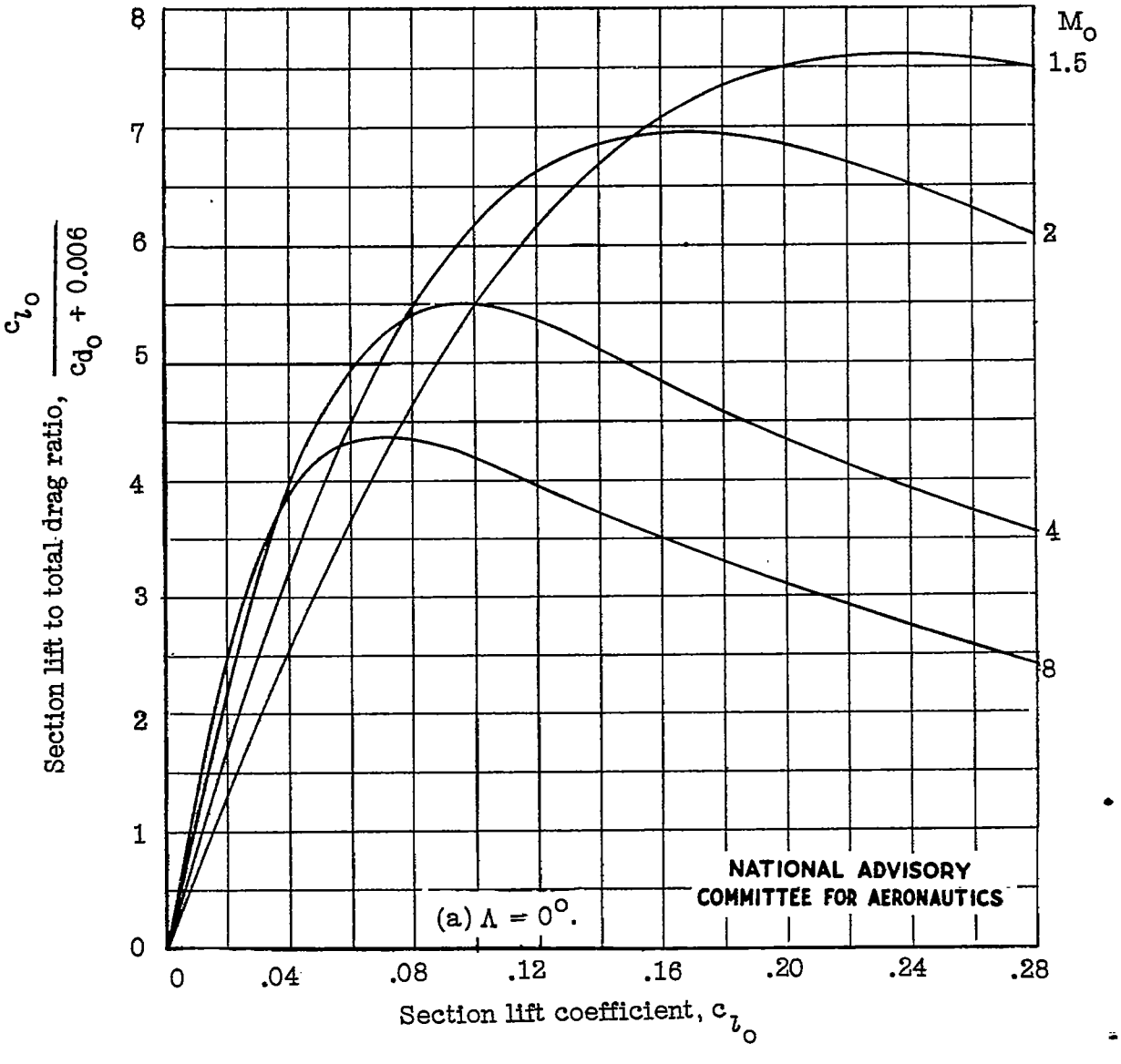

Figure 15.- Ratio of lift to total drag; $\left(\frac{t}{c}\right)_o = 0.05$.

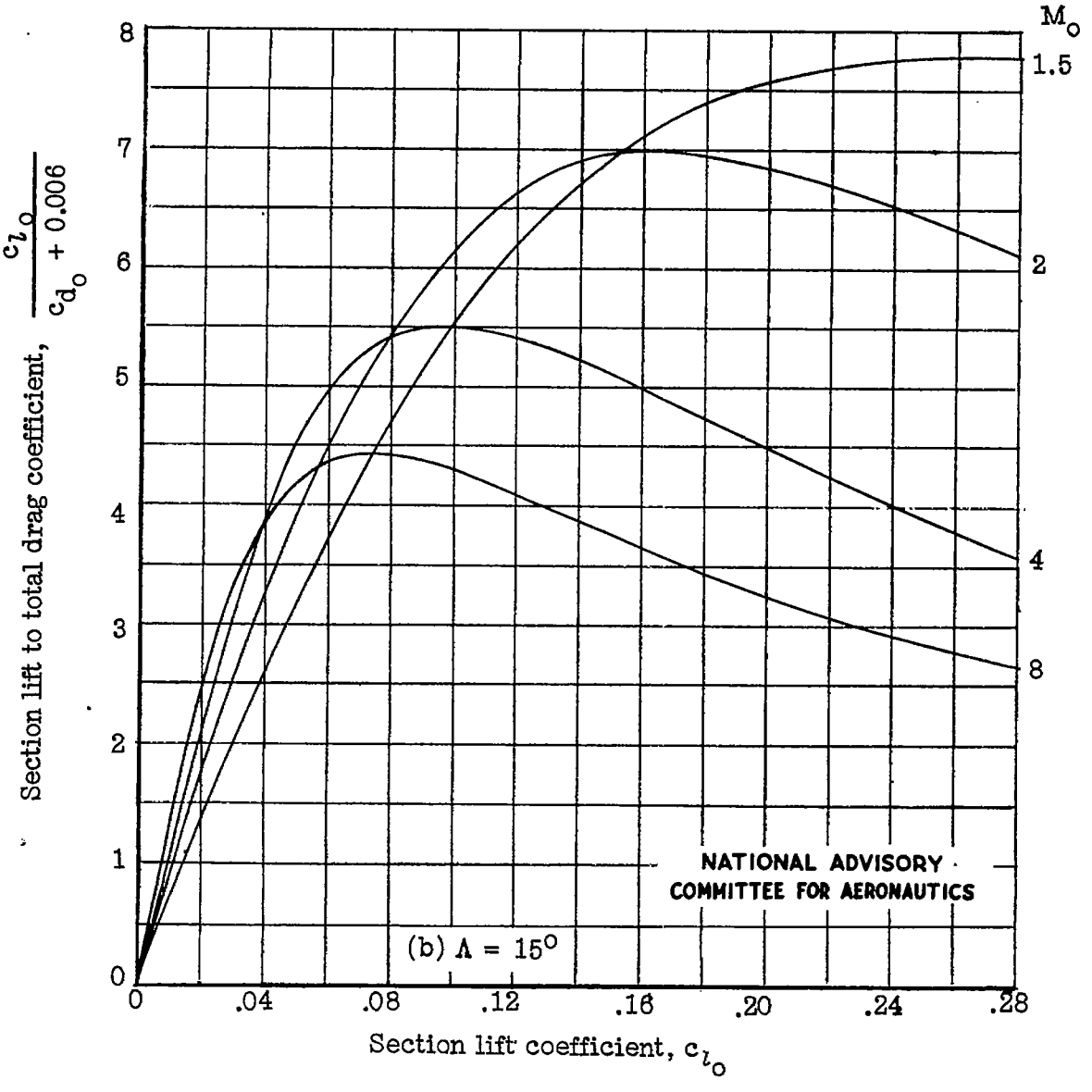

Figure 15.- Continued.

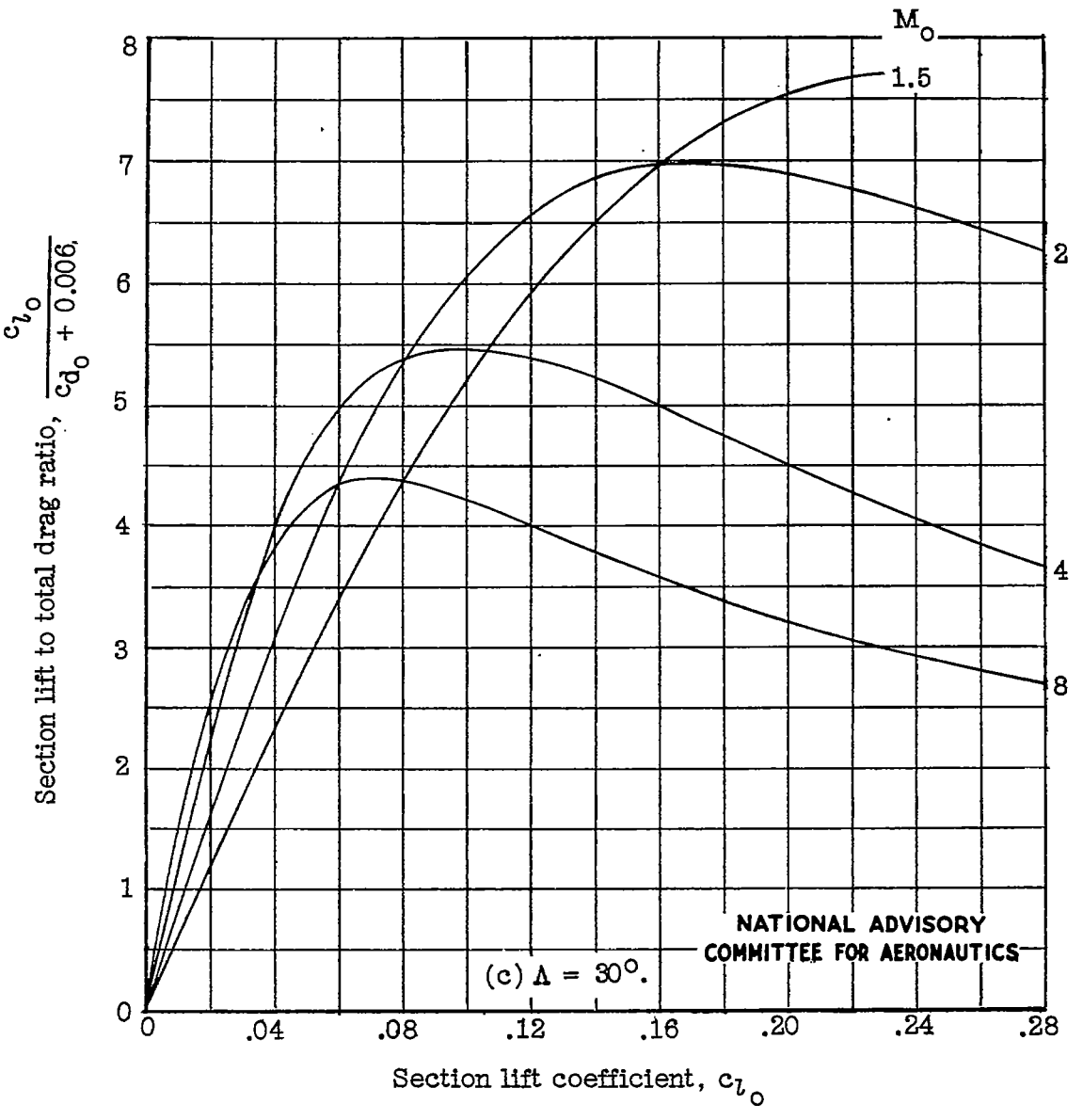

Figure 15.- Continued.

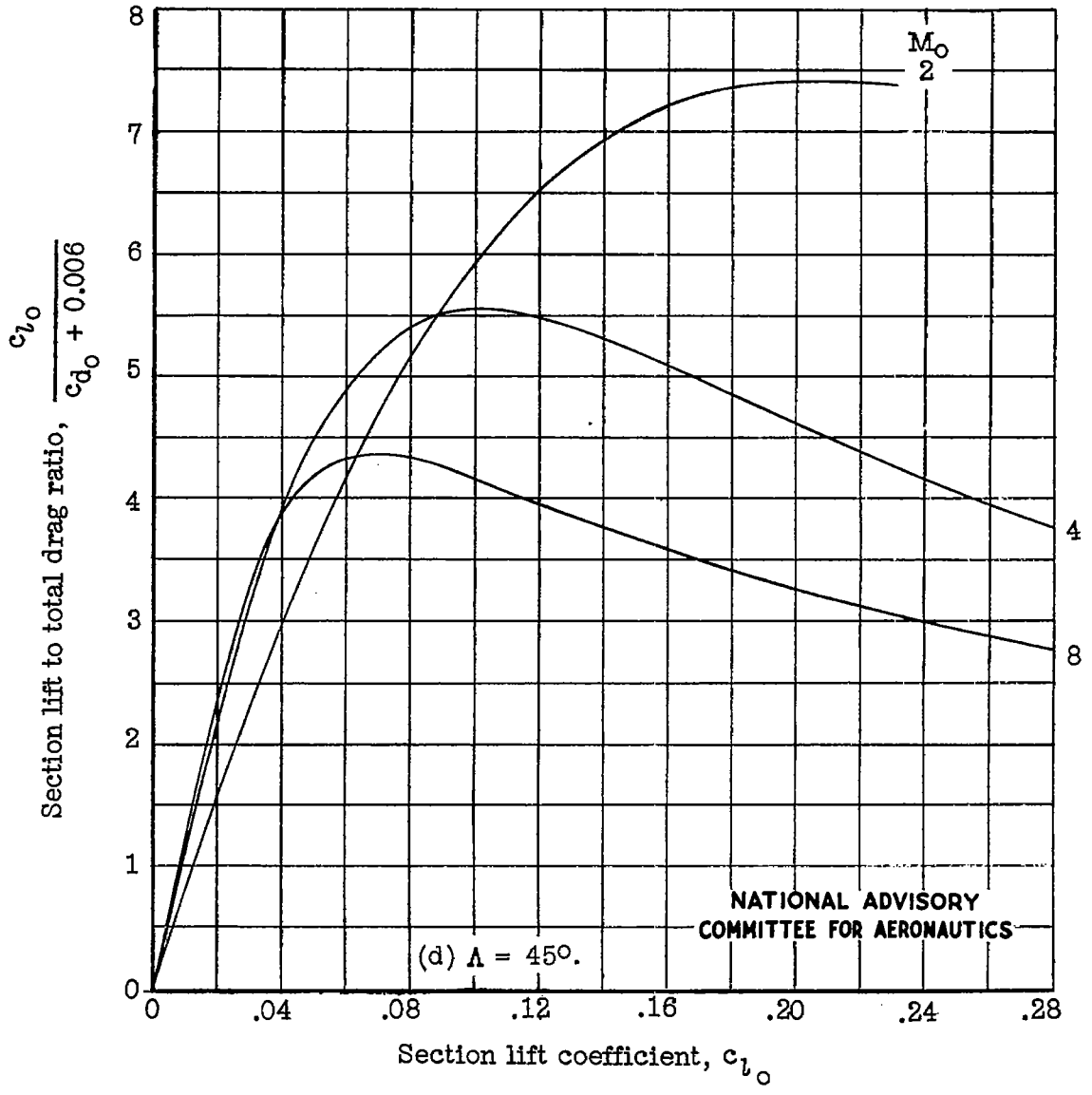

Figure 15.- Continued.

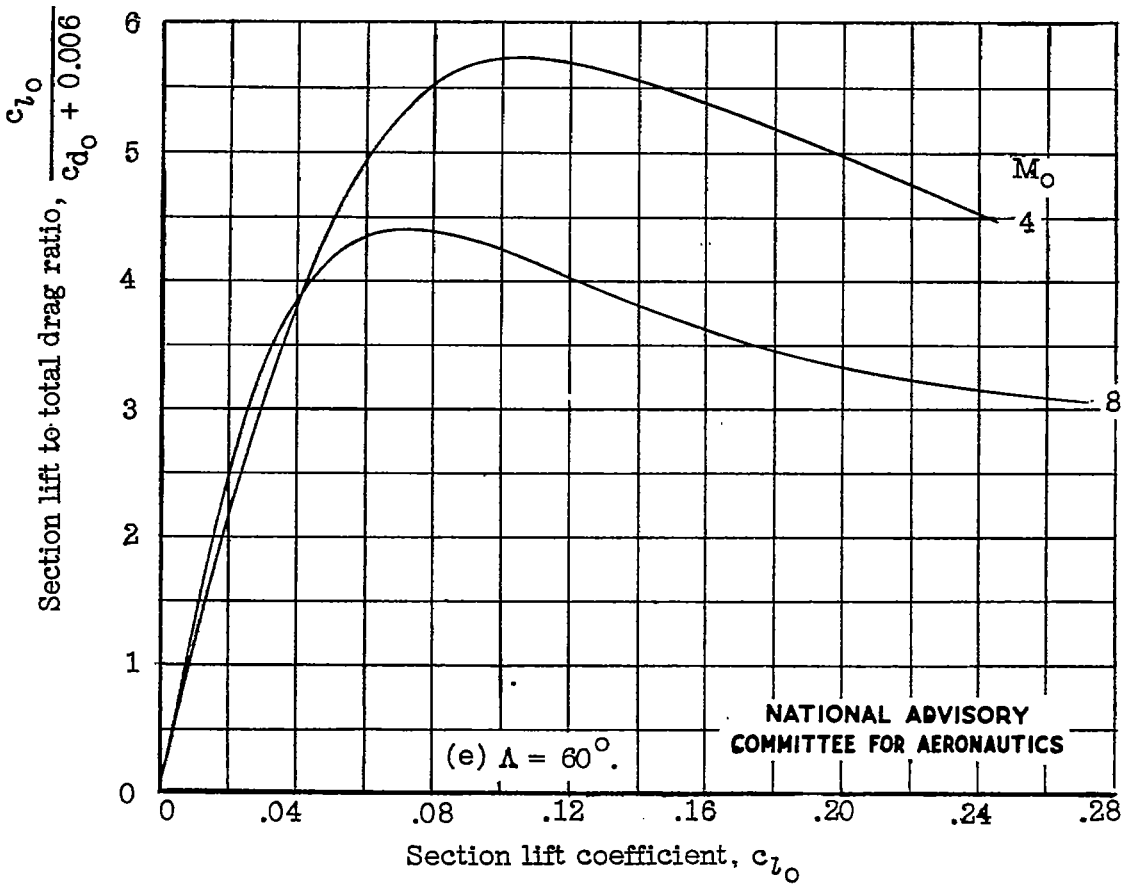

Figure 15.- Concluded.

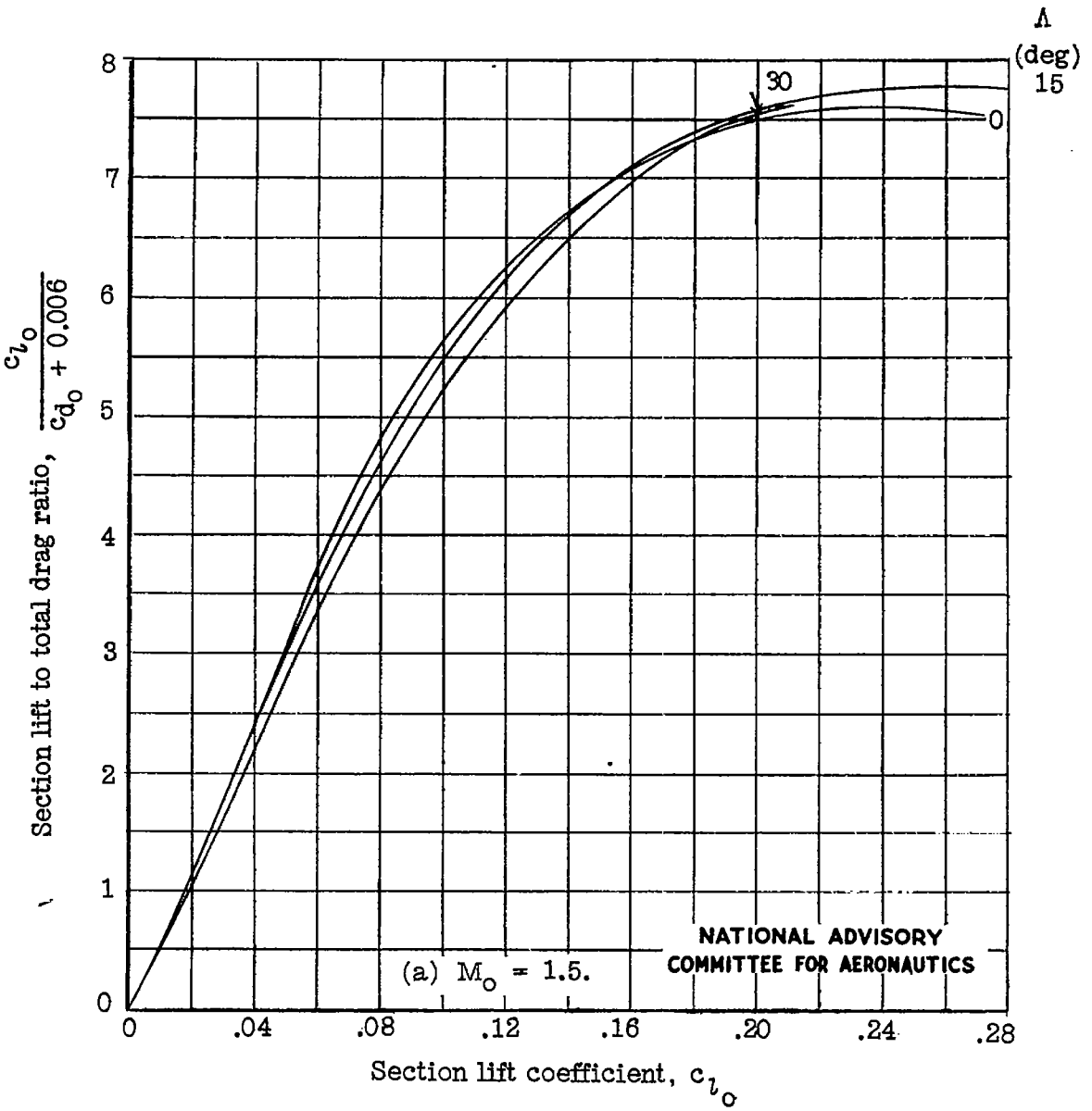

Figure 16.- Lift to total drag ratio; $\left(\frac{t}{c}\right)_o$ = 0.05.

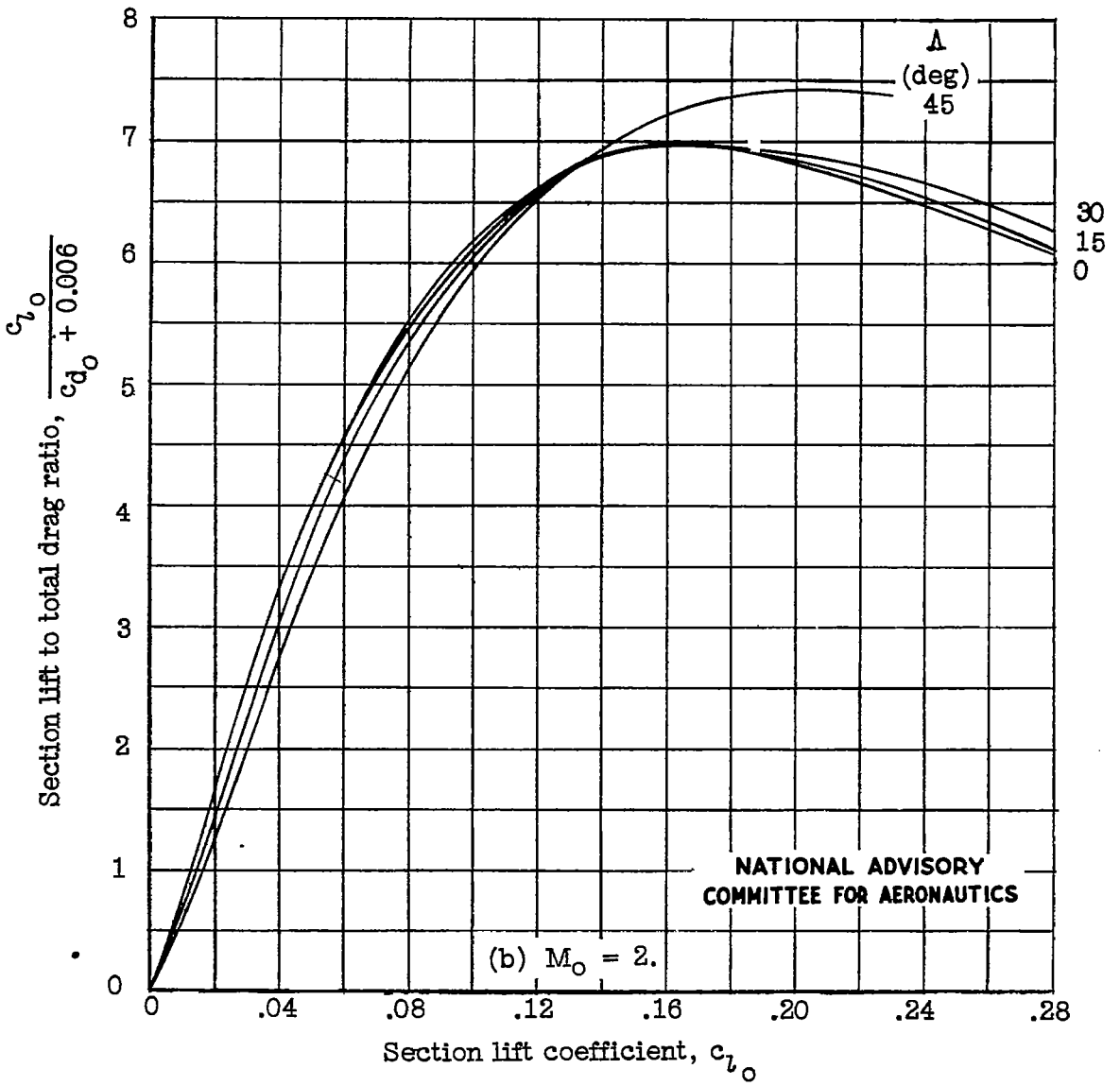

Figure 16.- Continued.

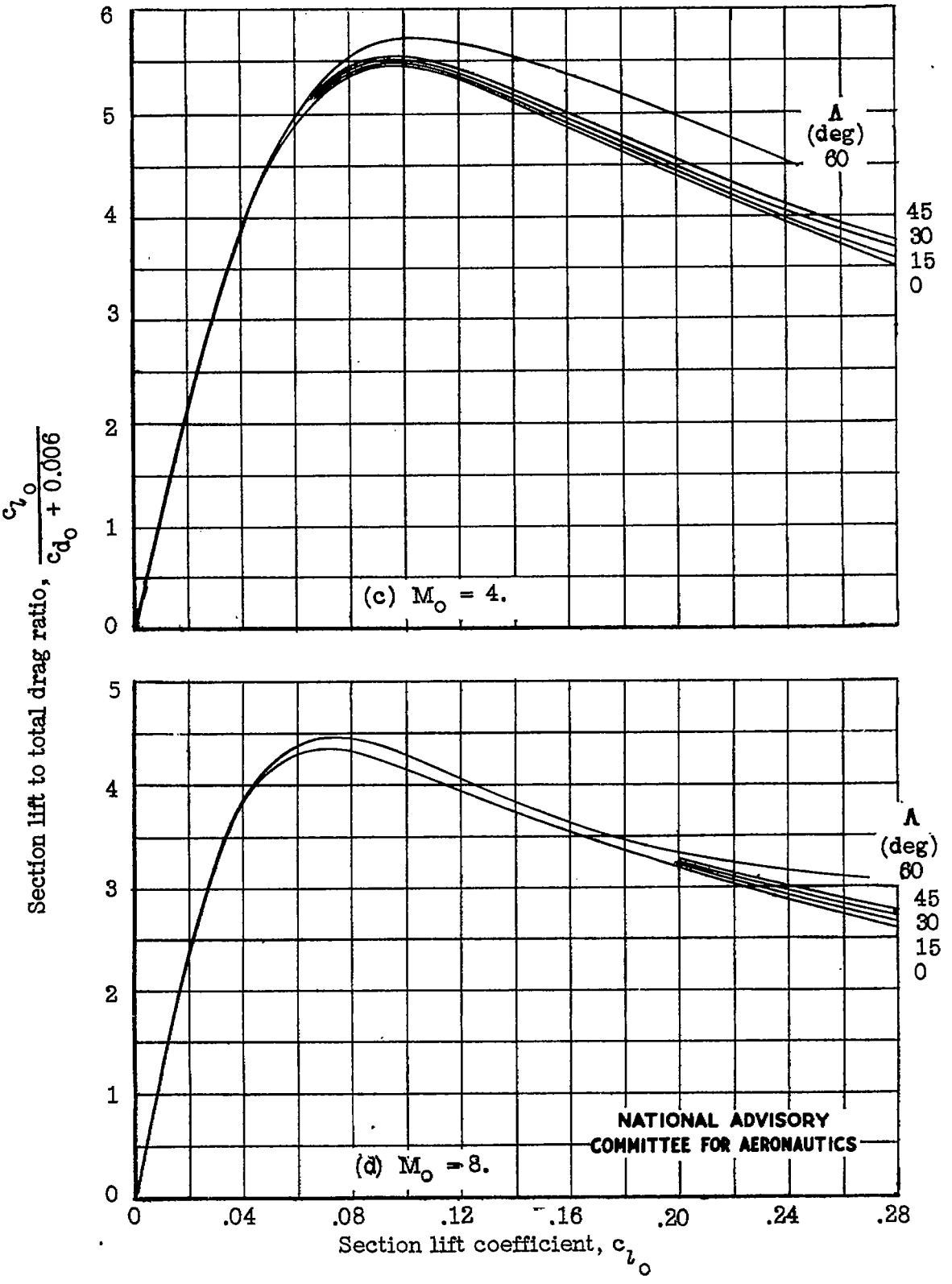

Figure 16.- Concluded.